Tuning of human MAIT cell activation by commensal bacteria species and MR1 dependent T cell presentation

Cihan Tastan[1,2], **Ece Karhan**[1], **Wei Zhou**[1], **Elizabeth Fleming**[1], **Anita Y. Voigt**[1], **Xudong Yao**[3], **Lei Wang**[3], **Meghan Horne**[1], **Lindsey Placek**[1], **Lina Kozhaya**[1], **Julia Oh**[1,#], and **Derya Unutmaz**[1,#]

[1]Jackson Laboratory for Genomic Medicine, Farmington, CT, 06032

[2]Department of microbiology, NYU School of Medicine, New York, NY, 10016

[3]Department of Chemistry, University of Connecticut, Storrs, CT, 06269

Abstract

Human mucosal-associated invariant T (MAIT) cell receptors (TCRs) recognize bacterial riboflavin pathway metabolites through the MHC class 1-related molecule MR1. However, it is unclear whether MAIT cells discriminate between many species of the human microbiota. To address this, we developed an *in vitro* functional assay through human T cells engineered for MAIT-TCRs (eMAIT-TCRs) stimulated by MR1-expressing antigen presenting cells (APC). We then screened 47 microbiota-associated bacterial species from different phyla for their eMAIT-TCR stimulatory capacities. Only bacteria species that encoded the riboflavin pathway were stimulatory for MAIT-TCRs. Most species that were high-stimulators belonged to *Bacteroidetes* and *Proteobacteria* phyla, whereas low/non-stimulator species were primarily *Actinobacteria* or *Firmicutes*. Activation of MAIT cells by high- vs low-stimulating bacteria also correlated with the level of riboflavin they secreted or after bacterial infection of macrophages. Remarkably, we found that human T cell subsets can also present riboflavin metabolites to MAIT cells in MR1- restricted fashion. This T-T cell mediated signaling also induced IFNγ, TNF and GranzymeB from MAIT cells, albeit at lower level than professional APC. These findings suggest that MAIT cells can discriminate and categorize complex human microbiota through computation of TCR signals depending on antigen load and presenting cells, and fine-tune their functional responses.

Introduction

Mucosal-associated invariant T (MAIT) cells are an innate-like T cell subset abundant in human blood and mucosal tissues like the liver and intestine[1–4]. MAIT cells are phenotypically defined by the expression of a semi-invariant T cell receptor (TCR) (Vα7.2 in humans) and the expression of CD161[1, 2] MAIT cells can be activated by cells that are infected with different bacterial species and yeast[3–7]. Analyses of germ-free mice reconstituted with different bacterial species suggest that commensal flora may be necessary for both the expansion of MAIT cells in the periphery and the acquisition of a memory phenotype[2,4,5]

It is now well-established that in both mice and humans, MAIT-TCR is stimulated through the MHC-Class I like molecule MR1 bound to metabolites from the bacterial riboflavin pathway[8–10]. A wide range of bacterial species contain this riboflavin pathway, several of which, such as *Mycobacterium (M.) tuberculosis, Escherichia (E.) coli* and *Staphylococcus (S.) aureus,* have been shown to stimulate MAIT cells[3, 5, 8]. In contrast, bacteria that lack the genes for this riboflavin pathway, such as *Enterococcus faecalis,* do not stimulate MAIT cells[5, 11]. The specific and MR1-restricted recognition of riboflavin metabolites by MAIT cells have been shown in MAIT-TCR transgenic mice and engineered human Jurkat cell lines with invariant Va-Ja and variable Vβ segments[2, 5, 8, 11].

Although the role of MAIT cells in immune response is yet to be fully elucidated, they appear to play a protective role in some experimental bacterial-infection models[6, 12–14] For example, infection of MR1-knock out mice, where MAIT cells are absent, with *Klebsiella pneumoniae* resulted in a high mortality rate[15]. In contrast, Va19 MAIT-TCR transgenic mice that were infected with either *E. coli* or *M. abscessus* had lower bacterial loads relative to controls[5, 16]. Further, in *in vitro* studies MAIT cells were shown to have an efficient cytotoxic effector function for bacterially infected cells[12, 13]. In humans, MAIT cells increase in the lungs of patients infected with the pulmonary pathogen *M. tuberculosis* (TB) and accumulation was observed in several other bacteria infected tissues[3, 17, 18] In contrast to tissues, MAIT cell frequency in blood are generally reduced in humans with different bacterial infections[18–21]. Collectively, these findings suggest that the infections may induce MAIT cell activation and possibly recruitment to the inflamed tissues to help for clearance of bacterial pathogens.

Several observations suggest that MAIT cells may also play a role in regulating responses to microbiota in human gut or skin and during chronic inflammatory diseases. For example, MAIT cell frequency is frequently reduced in blood of patients with inflammatory diseases such as Crohn's disease, multiple sclerosis (MS) and rheumatoid arthritis, but increased in inflamed tissue relative to healthy controls suggesting active migration to site of inflammation[22–24]. The composition of the local microbiota, which could impact activation and recruitment of MAIT cells, also changes in the inflamed tissues of Crohn's disease and psoriasis[25–29]. MAIT cells were also found to be reduced in the blood of HIV-infected patients both in adults[30–34] and children[35], which display chronic inflammation partly due to perturbations in the gut mucosal immunity and microbiota[36–40]. However, it is not yet known whether MAIT cells respond to commensal human microbiota residing in mucosal

tissues or skin, as to date, only selective and mostly pathogenic bacterial species are known to specifically stimulate MAIT cells[3, 578 15].

As such, a major knowledge gap remains in our understanding of how MAIT cells discriminate and respond to the substantial variation in the commensal human microbiota versus pathogenic bacterial species. To address this question, we developed a highly sensitive functional *in vitro* assay, by expression of engineered MAIT-TCRs (eMAIT-TCR) in human conventional CD8+ T cells, to screen bacterial metabolites that may stimulate MAIT cells. We found that bacterial species from the *Bacteroidetes* and *Proteobacteria* phyla were significantly high eMAIT-TCR stimulators, whereas of *Firmicutes* phylum was low/ non-stimulators, despite having riboflavin biosynthetic pathway. We also discovered that primary human T cell subsets have the capacity to activate MAIT cells through bacterial metabolites and induce cytokine secretion, however at relatively lower strength of TCR-signals, which correlate with their low MR1 expression. Our study suggests that MAIT cells can sense the composition of microbiota species by tuning their TCR signals, in a manner dependent on metabolite concentrations from different commensal bacterial species and expression level of MR1 on presenting cells.

Results

Development of a functional assay for screening MAIT-TCR stimulation by bacteria

MAIT cell activation is mostly restricted to metabolites from bacterial riboflavin pathway, expressed by many bacterial species (both pathogenic and commensal). Thus, it remains unclear whether MAIT cells can discriminate between the composition of thousands of different commensal bacterial species in the human microbiota. However, screening hundreds or thousands of bacteria for their capacity to stimulate human MAIT cells is challenging due to their relatively small and highly variable frequency in human blood. To overcome this, we aimed to develop a robust functional assay that was highly sensitive, high-throughput, and could recapitulate activation of primary MAIT cells by diverse commensals or pathogenic bacterial species found in the human microbiota (Fig. 1A). Accordingly, we utilized a human EBV- transformed and transporter associated with antigen processing (TAP)-deficient B cell line called T2 cells[41] as antigen presenting cells (APC), which express MR1 on cell surface (Fig. 1B). To determine the role of MR1 in this assay, we either further overexpressed MR1 on T2 cells, or using CRISPR/Cas9 gene editing deleted *MR1* or *B2M* (β_2-microglobulin, β2m) gene (Fig. 1B), as cell-surface presentation of MR1 molecules requires expression of β2m[4] Wild type and MR1hi and MR1- T2 cells were pre-incubated with *E. coli* supernatant or tryptic soy broth (TSB) medium used for culturing *E. coli,* as control, washed and co-cultured with peripheral blood mononuclear cells (PBMC) for 24 hrs. Subsequently, activation of Vα7.2+CD161+ CD8+ MAIT cells in PBMC (Fig. 1C) was assessed by upregulation of CD25 and CD69 surface molecules (Fig. 1D). Both wild type T2 (T2-wt), which expresses MR1, and MRl-overexpressing T2 cells (T2-MR1hi) upregulated CD25 and CD69 expression specifically on CD8+ MAIT cells in PBMCs, although T2-MR1hi cells were more efficient, especially as *E. coli* supernatant was further diluted (Fig. 1D). In contrast, MAIT cells were not stimulated with either MRl-knockout T2 cells (T2-MR1−/−) pre-incubated with *E. coli* supernatant (Fig. 1D, bottom panel) or MR1-

expressing T2 cell lines with TSB controls (Fig. 1D), showing that specificity of activation is dependent on *E. coli* secreted metabolites and MR1 expression. We proceeded with subsequent experiments using T2-MR1hi cells as they were the most sensitive, likely due to increased capacity of MR1 to capture lower levels of metabolites in the bacterial supernatants.

Using PBMCs to screen hundreds or even thousands of bacterial species for specific MAIT stimulatory activity is highly challenging, due to large cell number requirements and donor-to- donor variation in MAIT-cell frequency and responses[1, 24] To overcome this, we engineered a MAIT cell specific TCR (eMAIT-TCR) with mouse TCRβ constant domain (mTCRβ), which avoids endogenous TCR mispairing, as previously described[42, 43] Accordingly, TCR-invariant Vα7.2 sequence with Jα33 gene segment was paired with TCR-Vβ2 domain conjugated with the Jβ2.1 *(TRBJ2–1)* segment (Fig. 2A) for its preferential usage with the dominant MAIT-TCR- Vβ2 [44–46] We then ectopically expressed this eMAIT-TCR on human conventional primary CD8+ T cells or a Jurkat cell line for comparison[8, 11]. The synthesized eMAIT-TCR Vα-Vβ gene construct was subcloned into a lentiviral vector, which contained GFP as a marker, and used to transduce the Jurkat cell line or activated purified human CD8+ T cells as previously described[43]. The Jurkat cell line or the expanded CD8+ T cells transduced with eMAIT-TCR- Vβ2 encoding vector co-expressed a GFP marker and as mentioned above, the mTCRβ, which can be stained with a specific antibody (Fig. 2B). Cells gated on mTCRβ+GFP+ subset expressed both Vα7.2 and Vβ2 parts of the eMAIT-TCR both in Jurkat or CD8+ T cells (Fig.2B) and only mTCRβ+ cells were stained with MR1–5-OP-RU tetramer (Fig. 2C), which specifically binds to MAIT-TCRs as described[11], and thus confirming this as MAIT-TCR.

Upon stimulation of eMAIT-TCR-Vβ2+ cells with T2-MR1hi cells pre-incubated with *E. coli* supernatant, Jurkat cells only induced CD69, whereas, primary CD8+ T cells expressing the eMAIT-TCR greatly upregulated both CD25 and CD69 expression (Fig. 3A). The eMAIT-TCR expressing T cells were also activated in a dose dependent manner by MAIT cell stimulating riboflavin metabolite (5-ARU) (Fig. S1). T2 cells lacking MR1 expression (either through *MR1* or *β2M,* which is required for MR1 expression expression[47, 48,]I gene-targeted CRISPR/Cas9 mediated deletion) did not activate eMAIT-TCR expressing cells either by *E. coli* supernatant or 5-ARU (Fig. 3B). Together, these findings conclusively show that the activation of eMAIT- TCR+ cells is MRl-dependent.

To demonstrate that eMAIT-TCR stimulation is also dependent on metabolites produced from riboflavin biosynthesis pathway of *E. coli,* we repressed the promoter element of *ribA* gene of the riboflavin pathway, by CRISPRi targeting in *E. coli* since *ribA* is required for production of MAIT-TCR stimulatory metabolites[49, 50]. Repression of *ribA* mRNA transcription was confirmed by qPCR and resulted in a reduced capacity of *E. coli* to stimulate eMAIT-TCR- expressing T cells (Fig. 3C). Further, *E. coli* growth time appeared to have little impact on MAIT stimulatory metabolite production since even 1 hour growth culture was sufficient for optimal stimulation of eMAIT-TCR+ T cells (Fig. S2).

As functional outputs for TCR-mediated activation, we also measured cytokine secretion and cytotoxicity from primary CD8+ T and Jurkat cell lines. Stimulation of eMAIT-TCR+

CD8+ primary T cells with *E. coli* supernatant induced high level of IFNγ secretion (Fig. 3D). The primary T cells expressing eMAIT-TCR also displayed high cytotoxicity against presenting T2- MR1^{hi} cells pre-cultured with either *E. coli* supernatant (Fig. 3E and 3F) or with 5-ARU metabolite (Fig. 3F). In contrast, these effector functions were not observed in the stimulated eMAIT-TCR-expressing Jurkat cells (Fig. 3D and 3F). Thus, these findings further validate that the primary T cells are both more sensitive for activation and display physiologically relevant effector functions upon eMAIT-TCR stimulation.

Screening of MAIT-TCR stimulation with diverse bacterial species

After establishing a proof-of-principle with να7.2+νβ2+ eMAIT-TCR, to expand the breadth of MAIT-TCR representation we engineered additional TCRs that contained the constant Vα7.2- Jα33 and Jβ2.1 but was paired with 20 different Vβ segments. These synthetic TCRs were individually expressed on CD8+ T cells and Jurkat cells, which were confirmed using Vβ- specific antibodies (Fig. S3). The TCR-engineered CD8+ primary T cells and Jurkat cells were then stained with MR1 tetramers pre-loaded either with 5-OP-RU or 6-FP as a negative control. Only 6 of the Vβ segments (Vβ 2, 12, 13.2, 13.5, 13.6, 20) bound MR1–5-OP-RU, albeit at differing levels (Fig. 4, A and B), possibly due to changes in overall TCR affinities. We then tested all TCRs for their capacity to signal in T cells using functional assay described above. We found that only 7 of the engineered-TCRs (all those stained with MR1–5-OP-RU and Vβ 13.1) were also stimulated by *E. coli* supernatant (Fig. 4C), and that staining intensity of these with MR1–5-OP-RU correlated with the proportion of cells activated (Compare Fig. 4B with 4C). In fact, the differences between strength of activation of these 7 eTCRs were much more evident when they were activated with varying concentrations of 5-ARU and activation was measured as IFNγ secretion (Fig. 4D), which showed remarkably similar hierarchy of Vβ MAIT-TCR activation both with *E. coli* supernatant and in MR1-tetramer staining intensity (Fig. 4D, middle and right panels). Henceforth, we refer to these 7 functional engineered-TCRs as eMAIT-TCRs, which were subsequently used in the functional bacterial screens as described below.

We next screened 47 human-associated bacterial species in the eMAIT-TCR assay for their stimulatory capacity. These were comprised primarily of commensals and belonging to different phyla present in different mucosal tissues as commensals, in addition to a few environmental strains potentially present in different human tissues (Fig. 5A, tissue localization column) based on 16S rRNA and shotgun metagenomic studies[51, 52]. The eMAIT-TCR with Vβ2 was the most sensitive for detecting stimulation with supernatants from the bacterial species, with more variable activation of other engineered TCRs, assessed by CD25 and CD69 (Fig. 5A, bars under each eMAIT-TCR). This was again consistent with their binding patterns to MR1-tetramers (Fig. 4A and 4B). Species that lacked riboflavin pathway also completely lacked stimulatory capacity for any of the eMAIT-TCRs (Fig. 5A, gray strip). To more broadly quantify the capacity of different bacteria for their eMAIT-TCR stimulatory capacity, we added the percent activation by each eMAIT-TCR for each species to create a cumulative stimulation index (Fig. 5B). This analysis showed remarkable clustering of bacterial species based primarily on phyla (Fig. 5B and 5C) despite significant phylogenetic distance between the species themselves. Indeed, species belonging to *Bacteroidetes* and *Proteobacteria* had statistically higher MAIT-TCR stimulation capacity

compared to species *Firmicutes* or *Actinobacteria* (Fig. 5C). Importantly, measuring activation, by representative bacterial supernatants from each phylum, of primary CD8+ MAIT cells in healthy adult PBMCs, from different donors, recapitulated their respective stimulatory capacity (Fig. 5D) and correlated with cumulative stimulation of eMAIT-TCR+ CD8+ T cells (Fig. 5E). These findings suggest that activation of eMAIT-TCRs by diverse bacterial supernatants reflects their stimulatory capacity for primary MAIT cells.

To rule out the possibility that the eMAIT-TCR or primary MAIT cell activation could be affected by different bacterial density or concentration, given different growth kinetics for each species, we counted each species at their stationary phase as described in methods. While there was nearly 3-log difference in concentration among different species, there was no significant correlation between the bacterial counts and eMAIT-TCR stimulation (Fig. 5F), which is also consistent with the time course experiment using *E. coli* cultures where metabolite concentrations quickly reached high levels sufficient for MAIT-TCR activation before stationary phase (Fig. S2).

These findings suggested that bacteria could possess the riboflavin pathway yet not synthesize sufficient levels of riboflavin or secrete the metabolites that are required for MAIT cell activation. To confirm this, we measured riboflavin secretion from a select group of high and low MAIT-stimulating bacteria that possessed the riboflavin pathway using mass spec analysis. Those lacking the pathway were used as controls. For this experiment, the bacteria were grown overnight and then washed to remove the media, counted and resuspended in PBS at similar numbers and incubated for an additional 2 hours. The mass spec analysis of riboflavin in bacterial supernatants were then performed as described in detail in methods section. Indeed, the high-stimulator bacteria species secreted greater amount of riboflavin compared to low- stimulator bacteria (Fig. 6A).

However, it is also possible that MR1-binding metabolites produced by some bacteria may not be as stable. To address this, we added bacteria directly on to primary human macrophages in the presence of human serum. In this assay, bacteria would be taken up by the macrophages and their metabolites then bind to MR1 in macrophages and be presented to eMAIT-TCR cells. We then measured secretion of IFNγ from the eMAIT-TCR cells after co-culturing with macrophages and bacteria. Remarkably, the activation of T cells as measured by IFNγ secretion again was greater with high- vs low-stimulator bacteria or those that lacked the riboflavin pathway (Fig. 6B). In a similar experimental approach, we also added the bacteria directly to PBMCs to test activation of primary MAIT cells. We found a similar activation profile, as assessed by specific upregulation of CD25 (Fig. 6C), only on primary MAIT cells with high- vs low-stimulator bacteria (Fig. 6D) but not in any non-MAIT CD8+ T cells which did not show any activation in the presence of the bacteria. To further confirm that this was MR1-dependent T cell activation, we used a blocking MR1 antibody which completely abolished the activation of primary MAIT cells compared to isotype control antibody (Fig. 6E). Together these findings suggest that, at least for the bacteria tested in these experiments, the level of riboflavin production is appeared to be the main driver of their capacity to stimulate MAIT cells.

Stimulation of MAIT-TCR by bacterial antigens in the absence of antigen presenting cells

During course of eMAIT-TCR stimulation assays, we observed that supernatants from high stimulatory bacteria *(E. coli* or *C. normanense)* could activate eMAIT-TCR expressing cells alone, that is in the absence of T2 cells (Fig. 7A and 7B). This was a surprising result and suggested that primary human T cells may express sufficient level of MR1 for T-T cell presentation of bacterial metabolites. Although expression of MR1 in primary T cells was very low, deletion of either *MR1* or *β2M* gene (as mentioned above, required for MR1 cell surface expression) using CRISPR/Cas9 gene editing in primary T cells resulted reduction in intensity of MR1 antibody staining (Fig. 7C). Furthermore, MR1 expression was increased upon incubation of the cells with 5-ARU (Figure S4), using a previously described protocol[53] suggesting that primary T cells can express MR1 on cell surface. Importantly, deletion of $β_2$m also allowed us to negatively sort the $β_2$m-deleted cells (Fig. 7D), to generate primary T cells completely devoid of MR1 cell surface expression. Indeed, we found that $β_2m^{-/-}$ sorted CD4+ or CD8+ T cell subsets, pre-incubated with the bacterial supernatants as antigen-presenting cells (Fig. 7E), did not stimulate eMAIT-TCR+ CD8+ T cells (Fig. 7F) or primary MAIT cells (Fig. 7G). This demonstrates that T cells express sufficient level of MR1 to present bacterial metabolites to trigger MAIT-TCRs.

We next compared three different bacterial species *(C. normanense, E. coli* and *B. subtilis)* with different MAIT-cell stimulatory capacity in the absence or presence of T2-MR1^{hi} cells. While both primary MAIT cells within CD8+ T cells or eMAIT-TCR+ T cells were stimulated in the presence or absence of T2-MR1^{hi} cells with *C. normanense* or *E. coli* supernatants, the activation level based on CD25 expression were higher in the presence of T2-MR1^{hi} cells. Activation of primary MAIT cells alone in the presence of *B. subtilis* was much lower or undetectable (Fig. 7H). These experiments using bacteria supernatants revealed a gradient of MAIT-TCR stimulation strengths from resting CD8+ T cells (primary MAIT) and effector eMAIT-TCR+ cells to T2 cells overexpressing MR1, that was also dependent on stimulation capacity of the bacterial species.

To better assess and compare the presenter capacity of primary T cells, we next repeated similar experiments using 5-ARU metabolite as the antigen. In these experiments, we further sorted CD4+ T cells into naive (CD45RO-CCR7+; TN) and memory (CD45RO+; TM) subsets, as previously described[54]. In addition, a portion of the CD4+ T cells were also activated using anti- CD3+anti-CD28 beads (Invitrogen) and expanded in IL-2 culture for two weeks to prepare effector T cells (TE). CD8+ T cells and B cells were also purified from the same donors using Dynabead (Invitrogen) positive selection. CD4+ T cell subsets and B cells were then incubated with different concentrations of 5-ARU for 4 hours, washed, and then added on to autologous PBMCs. In addition, we also added 5-ARU directly onto PBMCs or purified CD8+ T cells, which contain majority of primary MAIT cells. After 2 days, activation of primary MAIT cells within PBMC was determined through staining with MAIT cell markers and expression of CD25 and CD69 (Fig. 8A). Similar to bacterial supernatant stimulations, we found that T cell subsets pre-cultured with 5-ARU stimulated primary MAIT cells in a concentration-dependent manner (Fig. 8B). However, naive T cells required high concentration of 5-ARU and had the lowest capacity of activating MAIT cells, compared to memory or effector T cells (Fig. 8B). On the other hand, 5-ARU directly

applied to PBMCs (that contain APCs such as dendritic cells and macrophages) or presented by purified primary B cells was relatively stronger in MAIT cell activation compared with T cell subsets used as APCs (Fig. 8B). As expected T2 cells had the highest stimulatory capacity (Fig. 8B).

We next determined whether stimulation of MAIT cells through T cell presentation of metabolites would also induce effector functions and determined how this compared to B cells or direct addition to PBMC. Accordingly, in the same experiments described above, after co-culture of 5-ARU presenting cells with PBMC, MAIT cells were stained after 22 hours, with surface markers and for intracellular expression of TNF, Granzyme B (GzmB) and IFNγ. As shown in representative flow cytometer data (Fig. 8C), sizeable portion of MAIT cells expressed both GzmB and TNF, when 5-ARU was added directly to PBMC. Concordant with results from the cell surface activation (Fig. 8B), memory or effector T cells induced lower levels of GzmB, or TNF or IFNy compared to B cell presentation or direct activation of PBMC (Fig. 8C and 8D), and that GzmB or cytokine expression from naive T cells was either very low or undetectable (Fig. 8C and 8D). Taken together, we conclude that primary T cells, particularly memory and effector T cells have the capacity to stimulate MAIT cells in antigen-specific and MRl-restricted manner.

Discussion

MAIT cells selectively respond to a broad range of microorganisms that possess the biosynthetic pathway for riboflavin metabolism[3, 568] Because diverse bacterial species produce riboflavin metabolites, we hypothesized that MAIT cells can fine tune their activation through strength of TCR signaling. The *in vitro* MAIT-TCR activation assay we developed here enabled us to test nearly four dozen bacterial species from different phyla that were primarily commensals in the human microbiota, many of which are known colonizers of mucosal tissues or skin or pathogenic species. We found highly significant variance among bacterial species for their MAIT-TCR stimulatory capacity. Furthermore, we provide evidence that T cells can act as antigen presenting cells for antigen-specific activation of MAIT cells and tuning of their effector functions.

Remarkably, most bacterial species that encode the riboflavin pathway and stimulated eMAIT- TCR expressing T cells belonged primarily to the *Bacteroidetes* and *Proteobacteria* phyla; whereas those with the lowest or no stimulatory activity were mostly from *Firmicutes* and a few *Actinobacteria.* This dichotomy is striking because the distribution or proportion of these bacterial species within the human microbiota also shifts with life history and different disease states, and these shifts may correlate with changes in MAIT cells numbers and activity. For example, the ratio of *Bacteroidetes* to *Firmicutes* species was found to be much higher in the infant gut microbiota compared to adults, and this composition skews toward an adult configuration within the first few years of life[55]. Therefore, our findings on higher MAIT-TCR stimulatory capacity of *Bacteroidetes* relative to *Firmicutes* would be consistent with the notion that they may drive expansion of MAIT cells after birth. We also note that *Cloacibacterium spp.,* species with the highest stimulatory capacity in our assay, have also been detected in breast milk samples of healthy women[56], which is one mechanism by which *Bacteroidetes* and other microbiota are established in the intestinal

flora of infants. Moreover, the *Bacteroidetes-to- Firmicutes* ratio is particularly perturbed in patients with Crohn's disease, who exhibit an increased *Bacteroidetes-to-Firmicutes* ratio[25–27], as well as an increase in *Cloacibacterium spp.* in sub-mucosal intestinal tissues[57]. Importantly, biopsied inflamed tissues of Crohn's disease patients exhibit significantly higher frequency of MAIT cells than do healthy tissues, and the MAIT cells isolated from these patients secreted more pro-inflammatory IL-17 cytokine relative to the controls[22]. This correlation between increased *Bacteroidetes* levels and MAIT cell number and activity taken together with our findings that supernatants of *Bacteroidetes* species displayed the highest eMAIT-TCR stimulatory activity provides a striking hypothesis: we envision that the chronic inflammation that typifies Crohn's disease might arise from perpetual activation of MAIT cells by species of the *Bacteroidetes* phylum, including *Cloacibacterium spp.* in the gut. Thus, we speculate that the bacterial species from *Bacteroidetes* and *Proteobacteria* phyla play an important role in expansion, maturation and homeostasis of MAIT cells in healthy humans and perturbation and aberrant activation of MAIT cells in inflammatory diseases.

HIV infection is another example of such a shift in microbial dysbiosis especially in the gastrointestinal track, which is also a primary site for viral replication and critical for its pathogenesis[58]. Numerous reports have shown potential dysbiosis in gut microbiota during HIV infection[36–40]. Interestingly, we and others have found significant decrease in MAIT cells in HIV-infected subjects, both in adults[30–34] and children[35]. A recent study also found that compared to healthy controls, the proportion of *Firmicutes* species is increased and conversely, the proportion of *Bacteroidetes* is decreased in patients with HIV[59]. Thus, it is tempting to speculate that the increase in ratio of low-stimulator to high-stimulators *(Firmicutes* to *Bacteroidetes)* of MAIT cells in HIV infection could be one of the reasons for the observed decline of MAIT cells in the blood of HIV-infected subjects.

In addition to the gut, CD8+ MAIT cells have also been shown to be resident in normal skin and are thought to play a role in skin-associated inflammations, such as psoriasis and dermatitis herpetimorfis, likely due to their determined IL-17 secretion in inflamed tissues[60, 61]. Indeed, similar to Crohn's disease, patients with psoriasis show an increase in the relative abundance of Bacteroidetes *and* Proteobacteria *and a relative decrease in* Actinobacteria *and* Firmicutes compared to normal skin[28, 29]. Of interest, *Propionibacterium acnes,* a member of *Actinobacteria*, had low/no MAIT-stimulatory capacity in our assays, is decreased in relative abundance on psoriatic skin lesions[28, 62]. This is especially striking since *P. acnes* is a dominant commensal member of the human skin microbiota[63–65] and is thought to have a protective role in maintaining healthy skin[28]. However, *P. acnes* can also cause acne when dysbiotic in oily intra- follicular skin sites[65–67]. Studies of acne lesions showed that *P. acnes* induced secretion of IL-17 from infiltrated CD4+ or CD8+ T cells[68, 69]. Thus, it is conceivable that environmental signals specific to a pro-inflammatory environment induce the riboflavin pathway in *P. acnes*, consequently stimulating the MAIT population and causing an inflammatory reaction.

It is also plausible that the high donor-to-donor variation in MAIT cell frequencies, which can be up to 20-fold difference in healthy adults,[1, 2, 70–72] could result from variation in the *Bacteroidetes-to-Firmicutes* ratio of the donor microbiota. We suggest that an individuals' unique microbiota composition and dynamics, which vary over one's lifetime[55] and can

change dramatically in response to different life events like pathogen response or inflammation, could be a key determinant in setting the MAIT cell frequency. For example, changes in the abundance of *Bacteroidetes* and *Firmicutes* during adulthood could be a set point for MAIT cell frequency as a sensor for microbial community composition. This is also supported by studies showing that the absence of MAIT cells in germ-free mice could be reversed upon reconstitution of the mice with bacteria[4, 5]. In addition to composition of the microbiota, the quantitative and qualitative differences in the magnitude of MAIT-TCR stimulation and expression of MR1, may act to fine- tuner MAIT cell activation for personalized set points for their frequencies. In this regard, it was surprising that majority of Vβ segments paired with canonical invariant MAIT-TCR, Va7.2 and Ja3 3 [71, 72], were non-functional. We speculate that this may partly be due to Jβ segment, which we kept constant for practical purposes. However, the functional eMAIT-TCRs with Vβ2 (TRBV20–1) and Vβ13 (TRBV6) segments in our assay are also highly represented within primary MAIT cells suggesting that these Vβ families form higher affinity MAIT-TCR in recognition of MR1 with the antigen[46,70,73]. Indeed, it has been suggested that TCR beta domain preferences may have been affected by various antigens from different microorganisms or pathogens and TCR beta recognition affinities[5, 44, 74–78]. For example, in cases of strong stimulators, such as *C. normanense,* more diverse Vβ recombined eMAIT-TCRs may be stimulated compared to low-stimulator bacteria species. It is also possible that different Vβ-Jβ segments that are present at lower frequencies within MAIT cells provide an additional facet of modulation, with different strength of signals via more diverse and/or rarer metabolites. Functional analysis of the MAIT cells, their TCR repertoire and composition of bacterial ecosystem in large set of individuals - especially in inflammatory diseases - would be valuable in future studies to address these possibilities.

A puzzling and striking observation from our screening assay was that many species that encode the riboflavin biosynthetic pathway in their genomes produced low levels of riboflavin and correspondingly did not exhibit eMAIT-TCR stimulatory activity. One possible explanation is of this diversity of the MAIT response to the bacterial species is that low-stimulatory species may only express riboflavin pathway genes under specific micro-environmental conditions or spatial distribution *in vivo* that were not mimicked in our *in vitro* cultures. This would provide an additional important potential regulatory mechanism for bacteria-MAIT activation that is based on environmental sensing pathways and the microbial milieu. For example, some *Firmicutes* and *Actinobacteria* possess putative riboflavin transporter systems that could potentially bypass the need for *de novo* synthesis of riboflavin, which is regulated by flavin nucleotide riboswitch if riboflavin is present in the environment[79, 80]. It is also worth noting that almost half of *Firmicutes* (130 genomes) and most *Actinobacteria* species (21 of 23 genomes) do not encode the riboflavin pathway[80], which would predict that, regardless these species have none or very low MAIT cell stimulatory capacity. Another possibility is that there may be some intraspecies diversity such that, different strains can possess unique variants that alter their MAIT stimulatory capability. For example, riboflavin biosynthetic pathway is highly conserved across *Str. pneumoniae* isolates[81], genetic differences in riboflavin operon in the characterized genomes of *Str. pneumoniae* isolates were also identified and could affect the MAIT cell magnitude of response *in vitro* and *in vivo*[82]. Future *in vivo* studies, for example in humanized mouse

models, or assessing different *in vitro* culture conditions for each bacterial species, may also reveal novel conditions or molecular switches that modulate MAIT-stimulatory metabolite secretion.

While several studies have used engineered Jurkat cell lines to test bacteria specific MAIT-TCR stimulation, the engineered conventional primary T cells developed here recapitulated more physiologically relevant aspects of primary MAIT cells compared to Jurkat cell line[5, 8, 11] As such, compared to primary T cells transduced with MAIT-TCR, Jurkat cells did not produce significant cytokines and did not have cytotoxic effector function, when activated through the TCR via MR1+riboflavin metabolites. Jurkat cells also lacked the dynamic range or sensitivity in MR1-depenent activation compared to primary T cells. We believe our highly-sensitive and high-throughput eMAIT-TCR assay using primary human T cells described here may be more valuable and sensitive in screening hundreds or thousands of bacterial strains isolated from healthy individuals and patients with chronic inflammatory diseases.

Another unexpected and important finding of our study was that T cells have the direct capability to present bacterial metabolites to MAIT cells in an MR1-restricted fashion, even though MR1 expression in human T cell subsets is barely detectable in our experiments and as reported[53]. However, the strength of MAIT activation through T cell antigen-presentation was lower compared to professional APC, such as primary B cells or MR1 expressing T2 cells. Nevertheless, the activation signals from T cell presentation to MAIT cells were sufficient to induce low levels of pro-inflammatory cytokines (IFNγ and TNFa) and cytotoxicity associated molecule GranzymeB. It is also important to note that MR1-antigen presentation through this primary T cell-MAIT cell interaction was revealed only when presenting T cells are exposed to metabolites from high stimulator bacteria such as *E. coli*, or directly by higher concentrations of 5-ARU. This finding suggests a scenario where if the concentration of riboflavin metabolites from certain bacterial species in the mucosal tissues or site of inflammation reaches a threshold, this can recruit surrounding T cells as additional antigen-presenting cells. This may in turn amplify MAIT cell activation and effector functions propagate the inflammatory response, especially because professional APCs may be quickly killed due to MAIT cell cytotoxicity. Indeed, other mucosal cell types such as lung epithelial cells can also express MR1[3], suggesting that MR1 expression is ubiquitous and can be utilized by MAIT cells at high riboflavin metabolite concentrations. Alternatively, it remains to be determined whether this T-MAIT interaction may also be regulatory, due to lack of co-stimulatory signals, similar to conventional T cell activation[83, 84]. In summary, we show that MAIT cells can discriminate between MRl-restricted, bacteria- derived metabolites through their TCR signaling thresholds and that non-professional antigen presentation such as from MR1-expressing bystander T cells that can regulate their activation or functions. Our findings and the development of a robust and physiologically relevant MAIT- TCR stimulation assay, paves the way to further elucidate how MAIT cells, akin to other immune cells[85], decode and are tuned by the complex and variable composition of the human microbiota. This knowledge is the first step in establishing a dynamic interactome and framework between MAIT cells and the human microbiota for the development of therapeutic approaches to maintain a healthy immunobiotic equilibrium.

Materials and Methods

PBMC and T cell purification

Healthy adult blood was obtained from New York Blood Center, New York, NY). PBMCs were isolated using Ficoll-paque plus (GE Health care). $CD4^+$ T, $CD8^+$ T, and $CD19^+$ B cells were purified using Dynal CD4 Positive, CD8 Positive and CD19 positive Isolation Kits (Invitrogen) respectively. $CD4^+$, $CD8^+$ T and CD19+ B cells were >99% pure as assessed by flow cytometry staining with respective antibodies. Purified $CD4^+$ T cells were sorted by flow cytometry (FACSAria; BD Biosciences) based on CD45RO expression into Naive T cells (CD4 TN) ($CD45RO^-$) and Memory T cells (CD4 TM) ($CD45RO^+$), sorted subsets were >98% pure. In some experiments, $CD4^+$ T cells were activated using anti-CD3/anti-CD28 coated beads (Invitrogen) and expanded for 2 weeks (TE). Cells were cultured at 37°C and 5% CO_2 in complete RPMI 1640 medium (RPMI supplemented with 10% Fetal Bovine Serum (FBS, Atlanta Biologicals), and 1% penicillin/streptomycin (Corning Cellgro).

Cell surface and intracellular staining and flow cytometry analysis.

Cells were resuspended in staining buffer (PBS + 2% FBS) and incubated with fluorochrome- conjugated antibodies for 30 min at 4°C. Stimulation of $eMAIT-TCR^+$ T cells was determined by staining with following antibodies: mouse constant TCRβ-PE (eBioscience), CD3-APC/Cy7, CD69-PerCP/Cy5.5, CD25-APC. Primary MAIT cell ($CD3^+CD8^+Va7.2^+CD161^+$) stimulation was also determined by staining with antibodies CD25, CD69 and CD4-BV605, CD8-A700, Va7.2-PE and CD161-BV421 (all from Biolegend). In cytotoxicity experiments, T2 cells were labeled with Cell Trace Violet (CTV) (Invitrogen) and pre-incubated with bacteria supernatant for 4 hours. After incubation, cells were washed and added to eMAIT cells. After 2 days, cells were stained with eFluor 506-conjugated Fixable viability dye (eBioscience) and eMAIT surface markers and then analyzed by flow cytometry. MR1 expression on T2 cells was assessed with anti-MR1-PE and β2m expression with anti$β_2$m-APC (all from Biolegend). Expression of eMAIT-TCRs was determined by expression of GFP, Va7.2 and respective Vβ antibody staining (kit from Beckman Coulter).

For intracellular cytokine staining, PBMCs were stimulated with the riboflavin metabolite 5-amino-4-D-ribitylaminouracil dihydrochloride (5-ARU, Toronto Research Chemicals, Canada) for 16 hours, then cultured additional 6 hours in the presence of GolgiStop (BD Biosciences). Cells were then washed and stained for surface markers using anti-CD3-Alexa Fluor 532 (eBioscience), anti-CD4-Pacific Blue, anti-CD8-Brilliant Violet 570, anti-Vα7.2-PE, anti- CD161- Brilliant Violet 421 and Fixable Viability Dye-eFluor 506 (Biolegend) and permeabilized, using a fixation/permeabilization buffer (eBioscience). Fixed cells were then stained intracellularly with anti-GzmB-Alexa Fluor 647, anti-TNFα-PE/Dazzle 594 and anti- IFNγ-APC.Cy7 (Biolegend). For MR1 blocking experiments, cells were pre-incubated with MR1 blocking antibody or mouse IgG2a isotype control (both from Biolegend) for 2 hours before stimulation with 5-ARU or bacteria.

Identification of MAIT cells with MR1 tetramers was described in previous study[11]. APC-conjugated human MR1 tetramers which are pre-loaded with either 5-OP-RU or 6-FP (negative control) were provided by NIH Tetramer Core Facility. Engineered MAIT-TCR expressing CD8+ T or Jurkat cells were stained with hMR1 tetramers for 40 min at room temp followed by mTCRβ surface staining for 30min. All flow cytometry analysis was performed using LSR Fortessa X-20 flow cytometer (BD Biosciences) or SP6800 (Sony) flow cytometer and analyzed using FlowJo software (Tree Star).

Preparation of bacteria supernatants

Bacterial strains were grown to stationary phase in the appropriate medium (Table S1) and centrifuged at 4000rpm to pellet the cells. The supernatants were then filtered through a 0.22- micron PES filter (EMD Millipore) to remove any remaining cells, and aliquoted for testing in the MAIT cell assay. Bacterial strains were obtained from the American Type Culture Collection (ATCC), DSMZ-German Collection of microorganisms and cell culture- and BEI Resources. Anaerobic bacterial species (marked * in Table S1) were grown in the anaerobic chamber (BACTRON, Shel Lab) with the conditions including 90% N_2, 5% H_2, 5% CO_2. *K. pneumoniae* strain was isolated from a patient by Bo Shopsin at New York University School of Medicine. *Staphylococcus epidermidis* Tu3298 was provided by Michael Otto at NIH.

Preparation of human macrophages and culture with bacteria

Monocytes were purified from PBMC of blood as previously described[86] and cultured with RPMI media with 5% human serum and GM-CSF for one day at 30 thousand cells/well in 96- well-plate. Selected bacteria were counted, centrifuged and resuspended in the RPMI +5% human serum media and added to macrophage cultures at varying numbers. After 4 hours of culture, eMAIT-TCR cells were added to the same cultures. After 2 days, IFNγ, was measured in the supernatants by a bead assay (Qbeads, Intellicyt) according to manufacturer's instructions and analyzed with iQue Screener plus (Intellicyt) flow cytometer.

CRISPR/Cas9 gRNAs and vectors.

LentiCRISPR_V2 (Addgene plasmid #52961)[87], was a gift from Feng Zhang. To generate gene- specific 20-nucleotide target sequences with minimum off-target scores, the online CRISPR design tool was used (which was developed by the Zhang Lab). The sequences were selected to precede 5'-NGG protospacer-adjacent motif (PAM) sequences. 20-nucleotide sequences 5'- GAACCTCGCGCCTGATCACT-3' and 5'-GAGTAGCGCGAGCACAGCTA-3' were designed to target the *MR1* gene and the *B2M* (β2m) gene, respectively. The oligonucleotides were purchased from Eurofins Genomics. Next, the oligonucleotides were annealed and cloned into the single guide RNA scaffold through Bsmbl-BsmbI sites in the LentiCRISPR_V2 vector. The cloned constructs were then transformed into NEB Stable Competent *E. coli* (New England Biolabs). The transformants were cultured overnight before plasmid DNA was isolated using QIAprep Spin Miniprep Kit and Qiacube (Qiagen). Successful cloning with the annealed oligo was confirmed by determining 2kb difference relative to the conventional LentiCRISPR_V2 vector that lacks the oligo after digesting the vectors with both Notl and BamHI restriction enzymes and

running on an agarose gel. Human MR1 transcript variant 1 (NM_001531) cDNA clone was purchased from Origene. The clone was then sub cloned into lentiviral vector encoding GFP marker[43].

Synthetic engineering and cloning of MAIT-TCRs.

Engineered TCRs were constructed as described in Figure 2A. Peptide sequences of the gene segments were downloaded from Ensembl Genome Browser. Transcript ID for each gene segment and sequences for p2A and Jβ2–1 linkages were listed in Table S2. The segments were connected in the following order: Vα7.2-Jα33-mTCRα-p2A-Vβ-Jβ2--mTCRβ, converted into a single open reading frame (ORF) and synthesized by Genscript. The synthesized eMAIT-TCR ORFs with each of the 21 different Vβ gene segments were sub-cloned into a lentiviral vector encoding GFP marker[43].

Lentiviral production and transduction.

The confirmed lentiviral constructs including MR1 or eMAIT-TCRs encoding vectors and the CRISPR constructs were co-transfected with the packaging plasmids VSVG, pLP1 and pLP2 into HEK293T cells using Lipofectamine™ 3000 (Invitrogen) according to the manufacturer's protocol. Lentiviral supernatants were collected, filtered and stored as previously described [44] Cell lines or primary T cells were transduced with lentiviruses line was infected with MOI of 1–5. For primary T cells, lentiviruses were added to purified CD8+ and CD4+ T cell subsets, which were stimulated using anti-CD3/anti-CD28 coated beads (Invitrogen) at 1:2 (bead: cell). After three days, the cells were selected either with 0.5–1 μg/ml puromycin antibiotic for 3–5 days until more than 95% of non-transduced cells were dead or sorted based on marker gene.

Bacteria counting

The Bacteria Counting Kit, which enumerates bacteria by flow cytometry, was purchased from Invitrogen (MP07277). The kit includes a nucleic acid stain that penetrates both gram-negative and gram-positive bacteria, producing green-fluorescent signal. The kit also includes a calibrated suspension of microspheres. Signals from both the stained bacteria and the beads were detected in the green fluorescence channel and were distinguished on a plot of forward scatter versus fluorescence using a flow cytometer. The density of the bacteria in the sample was determined from the ratio of bacterial signals to microsphere signals in the FACS plot as the commercial protocol suggests.

E. coli riboflavin gene knockout via CRISPR/Cas9

CRISPR approach was used to achieve gene knockdown. Respective *E. coli rib A* gene sequence was extracted from KEGG[88] including 100-nucleotide upstream of the start codon. Custom-made scripts were used to design spacers targeting the start sequence of the genes (non-template strand). The spacer oligos using primers (RibA_spacer_F, 5'-AAACGTTCTTCAAATCCCACCATCG and RibA_spacer_R, 5'-AAAACGATGGTGGGATTTGAAGAAC) were cloned into pdCas9 [50]. pdCas9 was a gift from Luciano Marraffini (Addgene plasmid # 46569). Spacer cloning into pdCas9 was carried out with 5-alpha competent *E. coli* (NEB) as described in Addgene spacer cloning

manual and the manufacturers manual. The transformed cells were plated on tryptic soy plates with chloramphenicol. Colonies were confirmed for the presence of the spacer in pCas9 plasmid using the primer pdCas9_f (5'-GTCTGAGCAAGAAATAGGCA) binding Cas9 and the respective reverse spacer pdCas9_r (5'-CGGAATGGACGATCACACTACTC) through PCR as well as a primer binding downstream of the integrated spacer pdCas9_r and the respective forward spacer. Positive colonies were grown overnight. For the eMAIT-TCR stimulation assay supernatants were obtained after centrifugation of the overnight culture for 5 min at 4000rpm followed by sterile filtration (0.2μm Fisherbrand Syringe Filters). Cell pellets were used for RNA extraction.

RNA isolation and rtPCR

E. coli overnight cultures were used to extract the RNA using the Qiagen RNAeasy kit. On-column DNase digestion step was carried out according to the manufacturer's manual. To improve purity of the RNA, a second round of DNase digestion was performed by adding 1μl of DNase to each 10μg of RNA eluted using the TURBO DNA-free Kit (ThermoFisher Scientific). After 30 min, another 1μl of DNase was added to the RNA and the reaction was quenched after 30 min according to the manufacturer's manual. Integrity of the RNA was checked on an agarose gel.

Reverse transcription was performed according to the manufacturer's instructions using the High-Capacity cDNA Reverse Transcription Kit (ThermoFisher Scientific). Per sample a reaction lacking the reverse transcriptase was included to account for DNA contamination. 0.4μg of RNA was used in each reaction. QRT-PCR primers (RibA-QPCR_F, 5'-CAGCTTAAACGTGTGGCAGA and RibA-QPCR_R, 5'-CGTCACCGGTCAGACATTC) were designed using the RealTime qPCR Assay tool from IDT and ordered from IDT. Off-target binding was checked by aligning the primer and spacer against the *E. coli* genome. Each sample was tested in replicates using the following protocol: 5μl 2x PowerUp SYBR Master Mix (Applied Biosystems), 0.25μM Primer mix (5μM), 2.25μl H2O and 2.5μl of RNA. RT-PCR was carried out using the ViiA-7 Real-Time PCR System (ThermoFisher Scientific). The *cysG* gene was used as the control housekeeping gene (CysG-QPCR-F, 5'-GGCGAAGAGCTGGAAACA and CysG-QPCR-R, 5'-CGTGAGTGGAATACCCGAATAG) and [89]. The Deltadelta CT- method implemented in the Quant-Studio Real-Time PCR Software (v1.1) was used to analyze the RT-PCR data.

Riboflavin pathway analysis

Riboflavin biosynthesis genes in bacteria whose genome sequences have been annotated by Kyoto Encyclopedia of Genes and Genomes (KEGG) were identified according to the annotation in KEGG pathway map00740. For unannotated bacterial genomes, riboflavin biosynthesis genes were identified in the following steps. First, all KEGG-annotated bacteria riboflavin biosynthesis genes (KEGG orthologues K01497, K01498, K02858, K00793 and K00794) were downloaded using the KEGG REST R package (version 1.14.0), and grouped according to KEGG orthology. Second, for each unannotated microbial genome, genes were predicted using PRODIGAL with default parameters [90]. Third, potential riboflavin biosynthesis genes were identified by aligning the KEGG-annotated riboflavin biosynthesis genes to the predicted genes using UBLAST[91], with parameters *evalue=1e-9* and *accel=0.6.*

Next, top hits from the blast search were validated using SMARTBLAST based on consistency in domain predictions. Finally, bacterial species that contain KEGG orthologues K01497, K01498, K02858, K00793 and K00794 are classified as species that have the riboflavin biosynthesis pathway.

Mass spectrometry quantitation of riboflavin in bacterial supernatants

Bacteria supernatant in PBS was acidified with 20% formic acid in water. Stable isotopic riboflavin-^{13}C,^{15}N$_2$ (VB2; Toronto Research Chemicals, Canada) was spiked as the internal standard. The spiked supernatants were desalted using an Oasis HLB 96-well μElution plate (Waters, Waltham, MA), following manufacturer's recommended procedures. Each sample was eluted with 50 μl of the elution solution, concentrated, and reconstituted to 20 μl with 0.2% formic acid in water. Riboflavin in each sample was quantified used the method of liquid chromatography-stable isotope dilution multiple reaction monitoring mass spectrometry (LC-SID-MRM MS)[92] with transitions of 377.15/172.10, 375.15/198.10, and 377.15/243.10 for positive ions of riboflavin and 380.10/173.11, 380.10/200.06, 380.10/246.07 for VB2. The column (Atlantis dC18, 5 μm, 0.3 mm x 150 mm; Waters, Waltham, MA) temperature was 40 °C. Solvent A was water/acetonitrile/formic acid = 98.8:1.0:0.2 (v/v/v), solvent B was water/acetonitrile/formic acid = 1.0:98.8:0.2 (v/v/v), and the flow rate was 9 μl/min. Each sample was analyzed in triplicate. Chromatograms were processed using the Skyline software and ratios of the peak area for riboflavin to that for VB2 were obtained. Original concentrations of riboflavin in bacterial supernatants were calculated using these ratios and the absolution concentration of VB2 in the analysis samples. Limit of quantitation for riboflavin was determined using the method of "blank and low-concentration samples"[93]. PBS treated with the same desalting procedure was used as the blank.

Statistical analysis

Correlation with the Spearman's rank test and two-tailed Mann-Whitney U tests were performed using GraphPad Prism software. No outliers were excluded in any of the statistical tests. Scatter dot plots report the median center lines with 25th and 75th quartile (interquartile range, IQR), and each data point represents an independent measurement. Correlation analysis was assessed with Spearman's rank test. Bar plots report the mean and standard deviation or the standard error of the mean. Threshold of significance for all tests was set at <0.05.

Supplementary Material

Refer to Web version on PubMed Central for supplementary material.

Acknowledgments:

References

1. Dusseaux M, Martin E, Serriari N, Peguillet I, Premel V, Louis D et al. Human MAIT cells are xenobiotic-resistant, tissue-targeted, CD161hi IL-17-secreting T cells. Blood 2011; 117(4): 1250–1259. [PubMed: 21084709]

2. Martin E, Treiner E, Duban L, Guerri L, Laude H, Toly C et al. Stepwise development of MAIT cells in mouse and human. PLoS Biol 2009; 7(3): e54. [PubMed: 19278296]

3. Gold MC, Cerri S, Smyk-Pearson S, Cansler ME, Vogt TM, Delepine J et al. Human mucosal associated invariant T cells detect bacterially infected cells. PLoS Biol 2010; 8(6): e1000407. [PubMed: 20613858]

4. Treiner E, Duban L, Bahram S, Radosavljevic M, Wanner V, Tilloy F et al. Selection of evolutionarily conserved mucosal-associated invariant T cells by MR1. Nature 2003; 422(6928): 164–169. [PubMed: 12634786]

5. Le Bourhis L, Martin E, Peguillet I, Guihot A, Froux N, Core M et al. Antimicrobial activity of mucosal-associated invariant T cells. Nat Immunol 2010; 11(8): 701–708. [PubMed: 20581831]

6. Meierovics A, Yankelevich WJ, Cowley SC. MAIT cells are critical for optimal mucosal immune responses during in vivo pulmonary bacterial infection. Proc Natl Acad Sci U S A 2013; 110(33): E3119–3128. [PubMed: 23898209]

7. Chua WJ, Truscott SM, Eickhoff CS, Blazevic A, Hoft DF, Hansen TH. Polyclonal mucosa-associated invariant T cells have unique innate functions in bacterial infection. Infect Immun 2012; 80(9): 3256–3267. [PubMed: 22778103]

8. Kjer-Nielsen L, Patel O, Corbett AJ, Le Nours J, Meehan B, Liu L et al. MR1 presents microbial vitamin B metabolites to MAIT cells. Nature 2012; 491(7426): 717–723. [PubMed: 23051753]

9. Patel O, Kjer-Nielsen L, Le Nours J, Eckle SB, Birkinshaw R, Beddoe T et al. Recognition of vitamin B metabolites by mucosal-associated invariant T cells. Nat Commun 2013; 4: 2142. [PubMed: 23846752]

10. Lopez-Sagaseta J, Dulberger CL, Crooks JE, Parks CD, Luoma AM, McFedries A et al. The molecular basis for Mucosal-Associated Invariant T cell recognition of MR1 proteins. Proc Natl Acad Sci U S A 2013; 110(19): E1771–1778. [PubMed: 23613577]

11. Corbett AJ, Eckle SB, Birkinshaw RW, Liu L, Patel O, Mahony J et al. T-cell activation by transitory neo-antigens derived from distinct microbial pathways. Nature 2014; 509(7500): 361–365. [PubMed: 24695216]

12. Le Bourhis L, Dusseaux M, Bohineust A, Bessoles S, Martin E, Premel V et al. MAIT cells detect and efficiently lyse bacterially-infected epithelial cells. PLoS Pathog 2013; 9(10): e1003681. [PubMed: 24130485]

13. Kurioka A, Ussher JE, Cosgrove C, Clough C, Fergusson JR, Smith K et al. MAIT cells are licensed through granzyme exchange to kill bacterially sensitized targets. Mucosal Immunol 2015; 8(2): 429–440. [PubMed: 25269706]

14. Cui Y, Franciszkiewicz K, Mburu YK, Mondot S, Le Bourhis L, Premel V et al. Mucosal-associated invariant T cell-rich congenic mouse strain allows functional evaluation. J Clin Invest 2015; 125(11): 4171–4185. [PubMed: 26524590]

15. Georgel P, Radosavljevic M, Macquin C, Bahram S. The non-conventional MHC class I MR1 molecule controls infection by Klebsiella pneumoniae in mice. Mol Immunol 2011; 48(5): 769–775. [PubMed: 21190736]

16. Ussher JE, Klenerman P, Willberg CB. Mucosal-associated invariant T-cells: new players in anti-bacterial immunity. Front Immunol 2014; 5: 450. [PubMed: 25339949]

17. Liuzzi AR, Kift-Morgan A, Lopez-Anton M, Friberg IM, Zhang J, Brook AC et al. Unconventional Human T Cells Accumulate at the Site of Infection in Response to Microbial Ligands and Induce Local Tissue Remodeling. J Immunol 2016; 197(6): 21952207. [PubMed: 27527598]

18. Jiang J, Wang X, An H, Yang B, Cao Z, Liu Y et al. Mucosal-associated invariant T-cell function is modulated by programmed death-1 signaling in patients with active tuberculosis. Am J Respir Crit Care Med 2014; 190(3): 329–339. [PubMed: 24977786]

19. Grimaldi D, Le Bourhis L, Sauneuf B, Dechartres A, Rousseau C, Ouaaz F et al. Specific MAIT cell behaviour among innate-like T lymphocytes in critically ill patients with severe infections. Intensive Care Med 2014; 40(2): 192–201. [PubMed: 24322275]

20. Smith DJ, Hill GR, Bell SC, Reid DW. Reduced mucosal associated invariant T-cells are associated with increased disease severity and Pseudomonas aeruginosa infection in cystic fibrosis. PLoS One 2014; 9(10): e109891. [PubMed: 25296025]

21. Leung DT, Bhuiyan TR, Nishat NS, Hoq MR, Aktar A, Rahman MA et al. Circulating mucosal associated invariant T cells are activated in Vibrio cholerae O1 infection and associated with lipopolysaccharide antibody responses. PLoS Negl Trop Dis 2014; 8(8): e3076. [PubMed: 25144724]

22. Booth JS, Salerno-Goncalves R, Blanchard TG, Patil SA, Kader HA, Safta AM et al. Mucosal-Associated Invariant T Cells in the Human Gastric Mucosa and Blood: Role in Helicobacter pylori Infection. Front Immunol 2015; 6: 466. [PubMed: 26441971]

23. Serriari NE, Eoche M, Lamotte L, Lion J, Fumery M, Marcelo P et al. Innate mucosal- associated invariant T (MAIT) cells are activated in inflammatory bowel diseases. Clin Exp Immunol 2014; 176(2): 266–274. [PubMed: 24450998]

24. Illes Z, Shimamura M, Newcombe J, Oka N, Yamamura T. Accumulation of Valpha7.2- Jalpha33 invariant T cells in human autoimmune inflammatory lesions in the nervous system. Int Immunol 2004; 16(2): 223–230. [PubMed: 14734607]

25. Cho YN, Kee SJ, Kim TJ, Jin HM, Kim MJ, Jung HJ et al. Mucosal-associated invariant T cell deficiency in systemic lupus erythematosus. J Immunol 2014; 193(8): 3891–3901. [PubMed: 25225673]

26. Wright EK, Kamm MA, Teo SM, Inouye M, Wagner J, Kirkwood CD. Recent advances in characterizing the gastrointestinal microbiome in Crohn's disease: a systematic review. Inflamm BowelDis 2015; 21(6): 1219–1228.

27. Walker AW, Sanderson JD, Churcher C, Parkes GC, Hudspith BN, Rayment N et al. High-throughput clone library analysis of the mucosa-associated microbiota reveals dysbiosis and differences between inflamed and non-inflamed regions of the intestine in inflammatory bowel disease. BMC Microbiology 2011; 11(1): 7. [PubMed: 21219646]

28. Andoh A, Imaeda H, Aomatsu T, Inatomi O, Bamba S, Sasaki M et al. Comparison of the fecal microbiota profiles between ulcerative colitis and Crohn's disease using terminal restriction fragment length polymorphism analysis. J Gastroenterol 2011; 46(4): 479–486. [PubMed: 21253779]

29. Drago L, De Grandi R, Altomare G, Pigatto P, Rossi O, Toscano M. Skin microbiota of first cousins affected by psoriasis and atopic dermatitis. Clin Mol Allergy 2016; 14: 2. [PubMed: 26811697]

30. Fahlen A, Engstrand L, Baker BS, Powles A, Fry L. Comparison of bacterial microbiota in skin biopsies from normal and psoriatic skin. Arch Dermatol Res 2012; 304(1): 15–22. [PubMed: 22065152]

31. Cosgrove C, Ussher JE, Rauch A, Gartner K, Kurioka A, Huhn MH et al. Early and nonreversible decrease of CD161++ /MAIT cells in HIV infection. Blood 2013; 121(6): 951–961. [PubMed: 23255555]

32. Wong EB, Akilimali NA, Govender P, Sullivan ZA, Cosgrove C, Pillay M et al. Low levels of peripheral CD161++CD8+ mucosal associated invariant T (MAIT) cells are found in HIV and HIV/TB co-infection. PLoS One 2013; 8(12): e83474. [PubMed: 24391773]

33. Eberhard JM, Hartjen P, Kummer S, Schmidt RE, Bockhorn M, Lehmann C et al. CD161+ MAIT cells are severely reduced in peripheral blood and lymph nodes of HIV- infected individuals independently of disease progression. PLoS One 2014; 9(11): e111323. [PubMed: 25369333]

34. Fernandez CS, Amarasena T, Kelleher AD, Rossjohn J, McCluskey J, Godfrey DI et al. MAIT cells are depleted early but retain functional cytokine expression in HIV infection. Immunol Cell Biol 2015; 93(2): 177–188. [PubMed: 25348935]

35. Leeansyah E, Ganesh A, Quigley MF, Sonnerborg A, Andersson J, Hunt PW et al. Activation, exhaustion, and persistent decline of the antimicrobial MR1-restricted MAIT- cell population in chronic HIV-1 infection. Blood 2013; 121(7): 1124–1135. [PubMed: 23243281]

36. Khaitan A, Kilberg M, Kravietz A, Ilmet T, Tastan C, Mwamzuka M et al. HIV-Infected Children Have Lower Frequencies of CD8+ Mucosal-Associated Invariant T (MAIT) Cells that Correlate with Innate, Th17 and Th22 Cell Subsets. *PLoS One* 2016; 11(8): e0161786. [PubMed: 27560150]

37. Gori A, Tincati C, Rizzardini G, Torti C, Quirino T, Haarman M et al. Early impairment of gut function and gut flora supporting a role for alteration of gastrointestinal mucosa in human immunodeficiency virus pathogenesis. J Clin Microbiol 2008; 46(2): 757–758. [PubMed: 18094140]

38. Round JL, Mazmanian SK. The gut microbiota shapes intestinal immune responses during health and disease. Nat Rev Immunol 2009; 9(5): 313–323. [PubMed: 19343057]

39. Vujkovic-Cvijin I, Dunham RM, Iwai S, Maher MC, Albright RG, Broadhurst MJ et al. Dysbiosis of the gut microbiota is associated with HIV disease progression and tryptophan catabolism. Sci Transl Med 2013; 5(193): 193ra191.

40. Lozupone CA, Li M, Campbell TB, Flores SC, Linderman D, Gebert MJ et al. Alterations in the gut microbiota associated with HIV-1 infection. Cell Host Microbe 2013; 14(3): 329–339. [PubMed: 24034618]

41. Nowak P, Troseid M, Avershina E, Barqasho B, Neogi U, Holm K et al. Gut microbiota diversity predicts immune status in HIV-1 infection. AIDS 2015; 29(18): 2409–2418. [PubMed: 26355675]

42. Henderson RA, Michel H, Sakaguchi K, Shabanowitz J, Appella E, Hunt DF et al. HLA- A2.1-associated peptides from a mutant cell line: a second pathway of antigen presentation. Science 1992; 255(5049): 1264–1266. [PubMed: 1546329]

43. Cohen CJ, Zhao Y, Zheng Z, Rosenberg SA, Morgan RA. Enhanced antitumor activity of murine-human hybrid T-cell receptor (TCR) in human lymphocytes is associated with improved pairing and TCR/CD3 stability. Cancer Res 2006; 66(17): 8878–8886. [PubMed: 16951205]

44. Wan Q, Kozhaya L, Imberg K, Mercer F, Zhong S, Krogsgaard M et al. Probing the effector and suppressive functions of human T cell subsets using antigen-specific engineered T cell receptors. PLoS One 2013; 8(2): e56302. [PubMed: 23437112]

45. Gold MC, McLaren JE, Reistetter JA, Smyk-Pearson S, Ladell K, Swarbrick GM et al. MR1-restricted MAIT cells display ligand discrimination and pathogen selectivity through distinct T cell receptor usage. J Exp Med 2014; 211(8): 1601–1610. [PubMed: 25049333]

46. Gherardin NA, Keller AN, Woolley RE, Le Nours J, Ritchie DS, Neeson PJ et al. Diversity of T Cells Restricted by the MHC Class I-Related Molecule MR1 Facilitates Differential Antigen Recognition. Immunity 2016; 44(1): 32–45. [PubMed: 26795251]

47. Lepore M, Kalinichenko A, Colone A, Paleja B, Singhal A, Tschumi A et al. Parallel T- cell cloning and deep sequencing of human MAIT cells reveal stable oligoclonal TCRbeta repertoire. Nat Commun 2014; 5: 3866. [PubMed: 24832684]

48. Aldemir H Novel MHC class I-related molecule MR1 affects MHC class I expression in 293T cells. Biochem Biophys Res Commun 2008; 366(2): 328–334. [PubMed: 18068122]

49. Yamaguchi H, Hashimoto K. Association of MR1 protein, an MHC class I-related molecule, with beta(2)-microglobulin. Biochem Biophys Res Commun 2002; 290(2): 722–729. [PubMed: 11785959]

50. Soudais C, Samassa F, Sarkis M, Le Bourhis L, Bessoles S, Blanot D et al. In Vitro and In Vivo Analysis of the Gram-Negative Bacteria-Derived Riboflavin Precursor Derivatives Activating Mouse MAIT Cells. J Immunol 2015; 194(10): 4641–4649. [PubMed: 25870247]

51. Bikard D, Jiang W, Samai P, Hochschild A, Zhang F, Marraffini LA. Programmable repression and activation of bacterial gene expression using an engineered CRISPR-Cas system. Nucleic Acids Res 2013; 41(15): 7429–7437. [PubMed: 23761437]

52. Oh J, Freeman AF, Program NCS, Park M, Sokolic R, Candotti F et al. The altered landscape of the human skin microbiome in patients with primary immunodeficiencies. Genome Res 2013; 23(12): 2103–2114. [PubMed: 24170601]

53. Human Microbiome Project C Structure, function and diversity of the healthy human microbiome. Nature 2012; 486(7402): 207–214. [PubMed: 22699609]

54. McWilliam HE, Eckle SB, Theodossis A, Liu L, Chen Z, Wubben JM et al. The intracellular pathway for the presentation of vitamin B-related antigens by the antigen- presenting molecule MR1. Nat Immunol 2016; 17(5): 531–537. [PubMed: 27043408]

55. Sundrud MS, Grill SM, Ni D, Nagata K, Alkan SS, Subramaniam A et al. Genetic reprogramming of primary human T cells reveals functional plasticity in Th cell differentiation. J Immunol 2003; 171(7): 3542–3549. [PubMed: 14500650]

56. Mariat D, Firmesse O, Levenez F, Guimaraes V, Sokol H, Dore J et al. The Firmicutes/ Bacteroidetes ratio of the human microbiota changes with age. BMC Microbiol 2009; 9: 123. [PubMed: 19508720]

57. Urbaniak C, McMillan A, Angelini M, Gloor GB, Sumarah M, Burton JP et al. Effect of chemotherapy on the microbiota and metabolome of human milk, a case report. Microbiome 2014; 2: 24. [PubMed: 25061513]

58. Chiodini RJ, Dowd SE, Chamberlin WM, Galandiuk S, Davis B, Glassing A. Microbial Population Differentials between Mucosal and Submucosal Intestinal Tissues in Advanced Crohn's Disease of the Ileum. PLoS One 2015; 10(7): e0134382. [PubMed: 26222621]

59. Mehandru S, Tenner-Racz K, Racz P, Markowitz M. The gastrointestinal tract is critical to the pathogenesis of acute HIV-1 infection. J Allergy Clin Immunol 2005; 116(2): 419–422. [PubMed: 16083799]

60. Ling Z, Jin C, Xie T, Cheng Y, Li L, Wu N. Alterations in the Fecal Microbiota of Patients with HIV-1 Infection: An Observational Study in A Chinese Population. Sci Rep 2016; 6: 30673. [PubMed: 27477587]

61. Teunissen MB, Yeremenko NG, Baeten DL, Chielie S, Spuls PI, de Rie MA et al. The IL-17A-producing CD8+ T-cell population in psoriatic lesional skin comprises mucosa- associated invariant T cells and conventional T cells. J Invest Dermatol 2014; 134(12): 2898–2907. [PubMed: 24945094]

62. Li J, Reantragoon R, Kostenko L, Corbett AJ, Varigos G, Carbone FR. The frequency of mucosal-associated invariant T cells is selectively increased in dermatitis herpetiformis. Australas J Dermatol 2016.

63. Gao Z, Tseng CH, Strober BE, Pei Z, Blaser MJ. Substantial alterations of the cutaneous bacterial biota in psoriatic lesions. PLoS One 2008; 3(7): e2719. [PubMed: 18648509]

64. Leeming JP, Holland KT, Cunliffe WJ. The microbial ecology of pilosebaceous units isolated from human skin. J Gen Microbiol 1984; 130(4): 803–807. [PubMed: 6234376]

65. Kong HH, Oh J, Deming C, Conlan S, Grice EA, Beatson MA et al. Temporal shifts in the skin microbiome associated with disease flares and treatment in children with atopic dermatitis. Genome Res 2012; 22(5): 850–859. [PubMed: 22310478]

66. Grice EA, Kong HH, Conlan S, Deming CB, Davis J, Young AC et al. Topographical and temporal diversity of the human skin microbiome. Science 2009; 324(5931): 1190–1192. [PubMed: 19478181]

67. Beylot C, Auffret N, Poli F, Claudel JP, Leccia MT, Del Giudice P et al. Propionibacterium acnes: an update on its role in the pathogenesis of acne. JEur Acad Dermatol Venereol 2014; 28(3): 271–278. [PubMed: 23905540]

68. Leyden JJ, McGinley KJ, Vowels B. Propionibacterium acnes colonization in acne and nonacne. Dermatology 1998; 196(1): 55–58. [PubMed: 9557227]

69. Kistowska M, Meier B, Proust T, Feldmeyer L, Cozzio A, Kuendig T et al. Propionibacterium acnes promotes Th17 and Th17/Th1 responses in acne patients. J Invest Dermatol 2015; 135(1): 110–118. [PubMed: 25010142]

70. Kelhala HL, Palatsi R, Fyhrquist N, Lehtimaki S, Vayrynen JP, Kallioinen M et al. IL- 17/Th17 pathway is activated in acne lesions. PLoS One 2014; 9(8): e105238. [PubMed: 25153527]

71. Held K, Beltran E, Moser M, Hohlfeld R, Dornmair K. T-cell receptor repertoire of human peripheral CD161hiTRAV1–2+ MAIT cells revealed by next generation sequencing and single cell analysis. Hum Immunol 2015; 76(9): 607–614. [PubMed: 26382249]

72. Tilloy F, Treiner E, Park SH, Garcia C, Lemonnier F, de la Salle H et al. An invariant T cell receptor alpha chain defines a novel TAP-independent major histocompatibility complex class Ib-restricted alpha/beta T cell subpopulation in mammals. J Exp Med 1999; 189(12): 1907–1921. [PubMed: 10377186]

73. Reantragoon R, Corbett AJ, Sakala IG, Gherardin NA, Furness JB, Chen Z et al. Antigen-loaded MR1 tetramers define T cell receptor heterogeneity in mucosal- associated invariant T cells. J Exp Med 2013; 210(11): 2305–2320. [PubMed: 24101382]

74. Kitaura K, Shini T, Matsutani T, Suzuki R. A new high-throughput sequencing method for determining diversity and similarity of T cell receptor (TCR) alpha and beta repertoires and identifying potential new invariant TCR alpha chains. BMC Immunol 2016; 17(1): 38. [PubMed: 27729009]

75. Gherardin NA, Keller AN, Woolley RE, Le Nours J, Ritchie DS, Neeson PJ et al. Diversity of T Cells Restricted by the MHC Class I-Related Molecule MR1 Facilitates Differential Antigen Recognition. Immunity 2016; 44(1): 32–45. [PubMed: 26795251]

76. Eckle SB, Birkinshaw RW, Kostenko L, Corbett AJ, McWilliam HE, Reantragoon R et al. A molecular basis underpinning the T cell receptor heterogeneity of mucosal- associated invariant T cells. J Exp Med 2014; 211(8): 1585–1600. [PubMed: 25049336]

77. Howson LJ, Napolitani G, Shepherd D, Ghadbane H, Kurupati P, Preciado-Llanes L et al. MAIT cell clonal expansion and TCR repertoire shaping in human volunteers challenged with Salmonella Paratyphi A. Nat Commun 2018; 9(1): 253. [PubMed: 29343684]

78. Dias J, Leeansyah E, Sandberg JK. Multiple layers of heterogeneity and subset diversity in human MAIT cell responses to distinct microorganisms and to innate cytokines. Proc Natl Acad Sci U S A 2017; 114(27): E5434–E5443. [PubMed: 28630305]

79. Lopez-Sagaseta J, Dulberger CL, McFedries A, Cushman M, Saghatelian A, Adams EJ. MAIT recognition of a stimulatory bacterial antigen bound to MR1. J Immunol 2013; 191(10): 5268–5277. [PubMed: 24108697]

80. Gutierrez-Preciado A, Torres AG, Merino E, Bonomi HR, Goldbaum FA, Garcia-Angulo VA. Extensive Identification of Bacterial Riboflavin Transporters and Their Distribution across Bacterial Species. PLoS One 2015; 10(5): e0126124. [PubMed: 25938806]

81. Magnusdottir S, Ravcheev D, de Crecy-Lagard V, Thiele I. Systematic genome assessment of B-vitamin biosynthesis suggests co-operation among gut microbes. Front Genet 2015; 6: 148. [PubMed: 25941533]

82. Kurioka A, van Wilgenburg B, Javan RR, Hoyle R, van Tonder AJ, Harrold CL et al. Diverse Streptococcus pneumoniae Strains Drive a Mucosal-Associated Invariant T-Cell Response Through Major Histocompatibility Complex class I-Related Molecule- Dependent and Cytokine-Driven Pathways. J Infect Dis 2018; 217(6): 988–999. [PubMed: 29267892]

83. Hartmann N, McMurtrey C, Sorensen ML, Huber ME, Kurapova R, Coleman FT et al. Riboflavin Metabolism Variation among Clinical Isolates of Streptococcus pneumoniae Results in Differential Activation of Mucosal-associated Invariant T Cells. Am J Respir Cell Mol Biol 2018; 58(6): 767–776. [PubMed: 29356555]

84. Zheng Y, Zha Y, Gajewski TF. Molecular regulation of T-cell anergy. EMBO Rep 2008; 9(1): 50–55. [PubMed: 18174897]

85. Smith TR, Verdeil G, Marquardt K, Sherman LA. Contribution of TCR signaling strength to CD8+ T cell peripheral tolerance mechanisms. J Immunol 2014; 193(7): 3409–3416. [PubMed: 25156361]

86. Pamer EG. Microbial Tuning of the Mammalian Immune System. Trends Mol Med 2017; 23(5): 379–380. [PubMed: 28372921]

87. Manel N, Hogstad B, Wang Y, Levy DE, Unutmaz D, Littman DR. A cryptic sensor for HIV-1 activates antiviral innate immunity in dendritic cells. Nature 2010; 467(7312): 214–217. [PubMed: 20829794]

88. Sanjana NE, Shalem O, Zhang F. Improved vectors and genome-wide libraries for CRISPR screening. Nat Methods 2014; 11(8): 783–784. [PubMed: 25075903]

89. Kanehisa M, Araki M, Goto S, Hattori M, Hirakawa M, Itoh M et al. KEGG for linking genomes to life and the environment. Nucleic Acids Res 2008; 36(Database issue): D480- 484. [PubMed: 18077471]

90. Zhou K, Zhou L, Lim Q, Zou R, Stephanopoulos G, Too HP. Novel reference genes for quantifying transcriptional responses of Escherichia coli to protein overexpression by quantitative PCR. BMC Mol Biol 2011; 12: 18. [PubMed: 21513543]

91. Hyatt D, Chen GL, Locascio PF, Land ML, Larimer FW, Hauser LJ. Prodigal: prokaryotic gene recognition and translation initiation site identification. BMC Bioinformatics 2010; 11: 119. [PubMed: 20211023]

92. Edgar RC. Search and clustering orders of magnitude faster than BLAST. Bioinformatics 2010; 26(19): 2460–2461. [PubMed: 20709691]

93. Ciccimaro E, Blair IA. Stable-isotope dilution LC-MS for quantitative biomarker analysis. Bioanalysis 2010; 2(2): 311–341. [PubMed: 20352077]

94. Mani DR, Abbatiello SE, Carr SA. Statistical characterization of multiple-reaction monitoring mass spectrometry (MRM-MS) assays for quantitative proteomics. BMC Bioinformatics 2012; 13 Suppl 16: S9.

95. Reantragoon R, Kjer-Nielsen L, Patel O, Chen Z, Illing PT, Bhati M et al. Structural insight into MR1-mediated recognition of the mucosal associated invariant T cell receptor. J Exp Med 2012; 209(4): 761–774. [PubMed: 22412157]
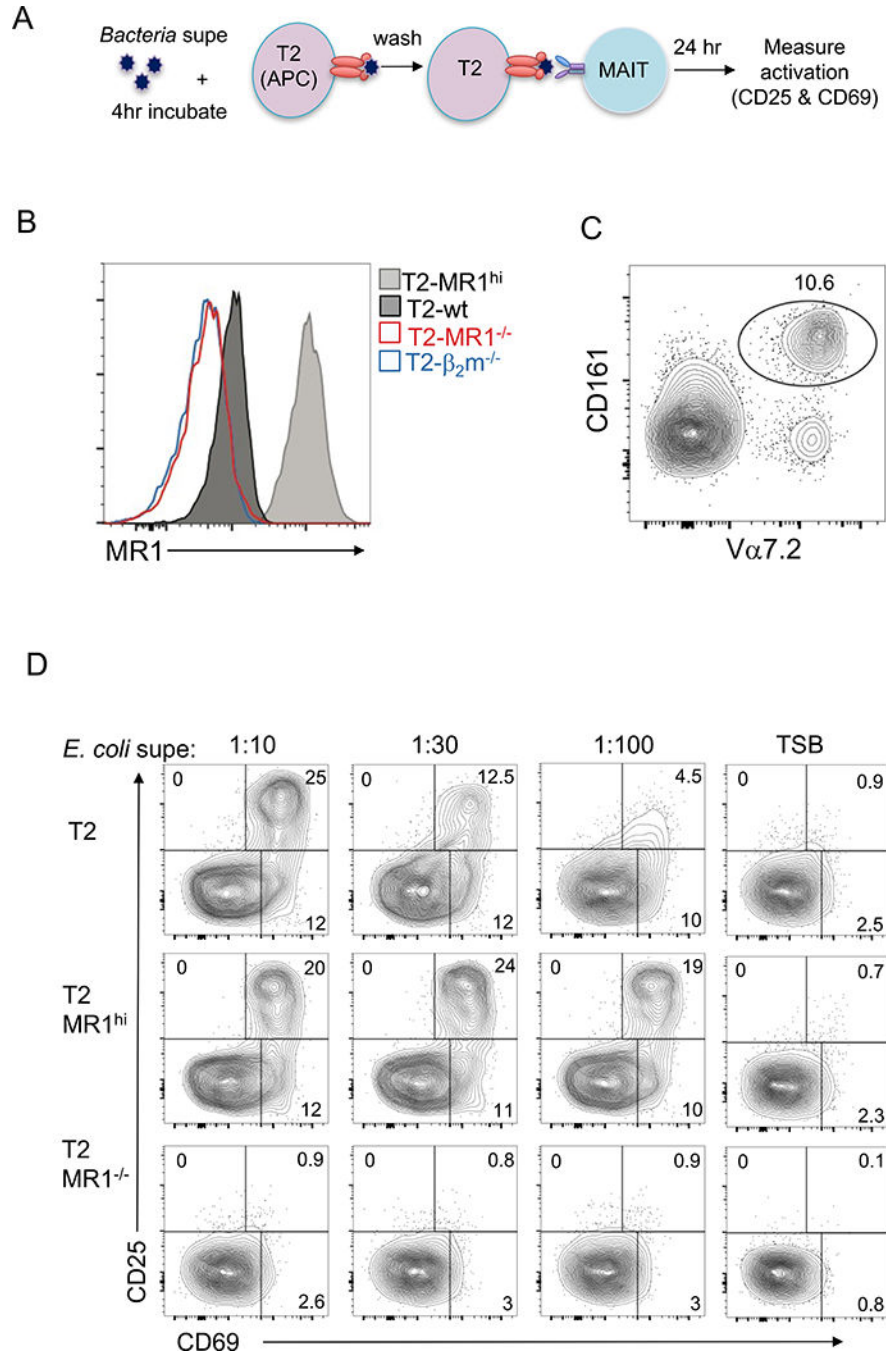
Figure 1. Stimulation of MAIT cells through MRl-expressing cells and bacterial supernatant.
(A) In this experimental approach, T2 cells were pre-incubated with *E. coli* supernatant or
TSB (mock) for four hours. The cells were then washed twice and cultured with human
adult PBMCs including MAIT cells for 16–24 hours. Activation of CD8+ MAIT cells was
determined by staining with antibodies against stimulation molecules CD25 and CD69. (B)
FACS plot of MR1 surface expression on MR1-overexpressing T2 (T2-MR1^{hi}, light gray
filled), wild type T2 (T2-wt, dark gray filled), MR1-knockout T2 (T2-MR1$^{-/-}$, empty red
line) and β2m- knockout T2 (T2-β$_2$m$^{-/-}$, empty blue line). (C) MAIT cell identification after

gating on CD3$^+$ CD8$^+$ Va7.2$^+$ CD161$^+$ cell subset. (D) CD25 and CD69 expression on CD8+ MAIT cells in PBMC cultured with the engineered T2 cell lines that were pre-incubated with either different dilutions of *E. coli* supernatant (1:10, 1:30 and 1:100) or TSB medium (1:10 dilution). Data is representative of at least three independent experiments with PBMCs from different healthy adult donors.
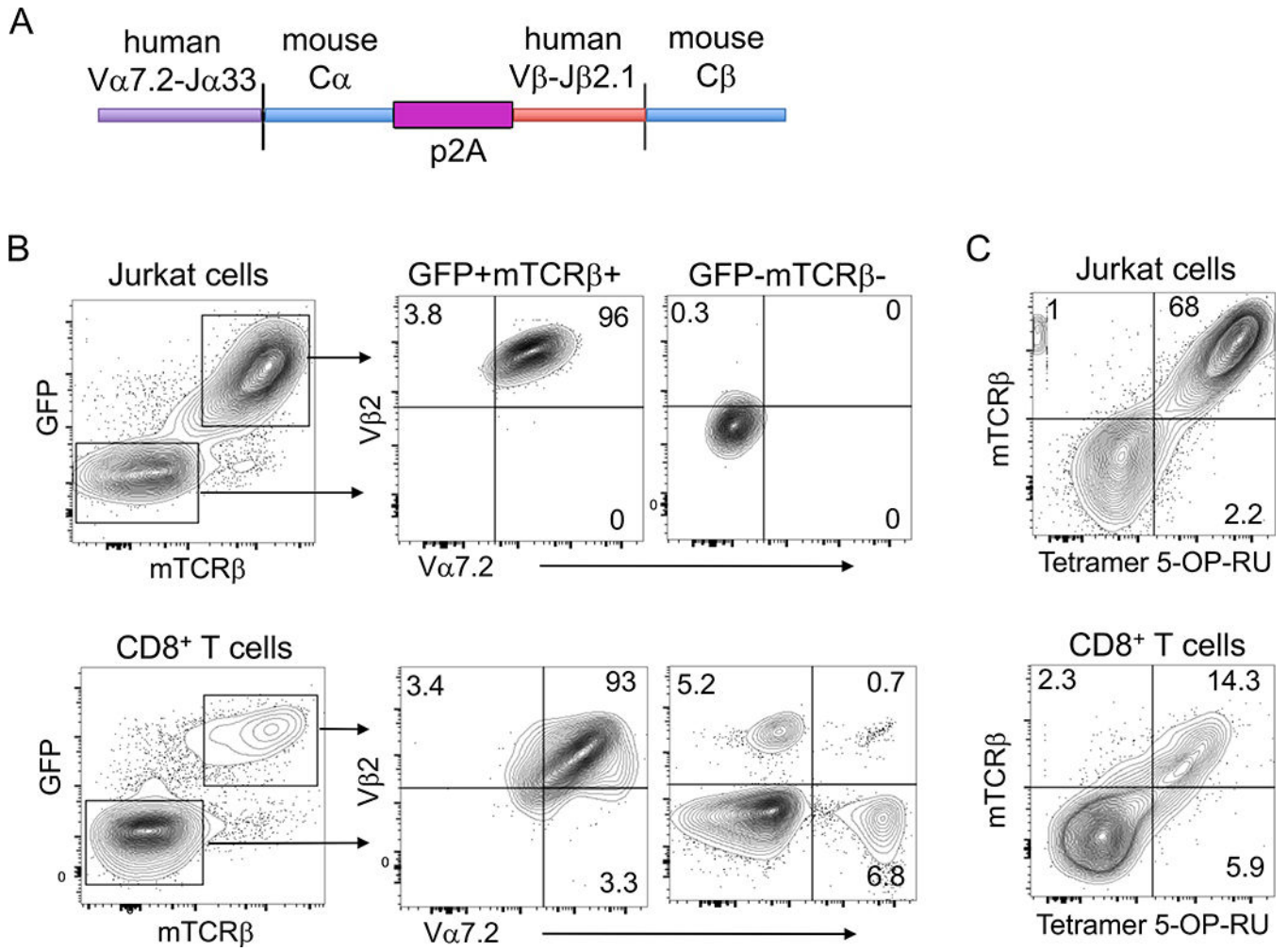
Figure 2. Development of MR1-restricted eMAIT-TCR expressing cells.
(A) Construction of eMAIT-TCRs. Human TCR Va7.2-Ja33 and Vβ-Jβ2.1 gene segments were combined with mouse TCR constant a and β segments, respectively and linked by a picornavirus-like 2A (p2A) self-cleaving peptide sequence. (B) Jurkat and primary human conventional CD8+ T cells that express either eMAIT-TCR-Vβ2 (GFP+mTCRβ+) or not (GFP-mTCRβ-), determined by staining with mTCRβ, Va7.2 and Vβ2 specific antibodies. (C) MR1-antigen complex specificity of the eMAIT-TCR+ cells determined by staining with 5-OP-RU pre-loaded APC-conjugated MR1 tetramer and anti-mTCRβ.
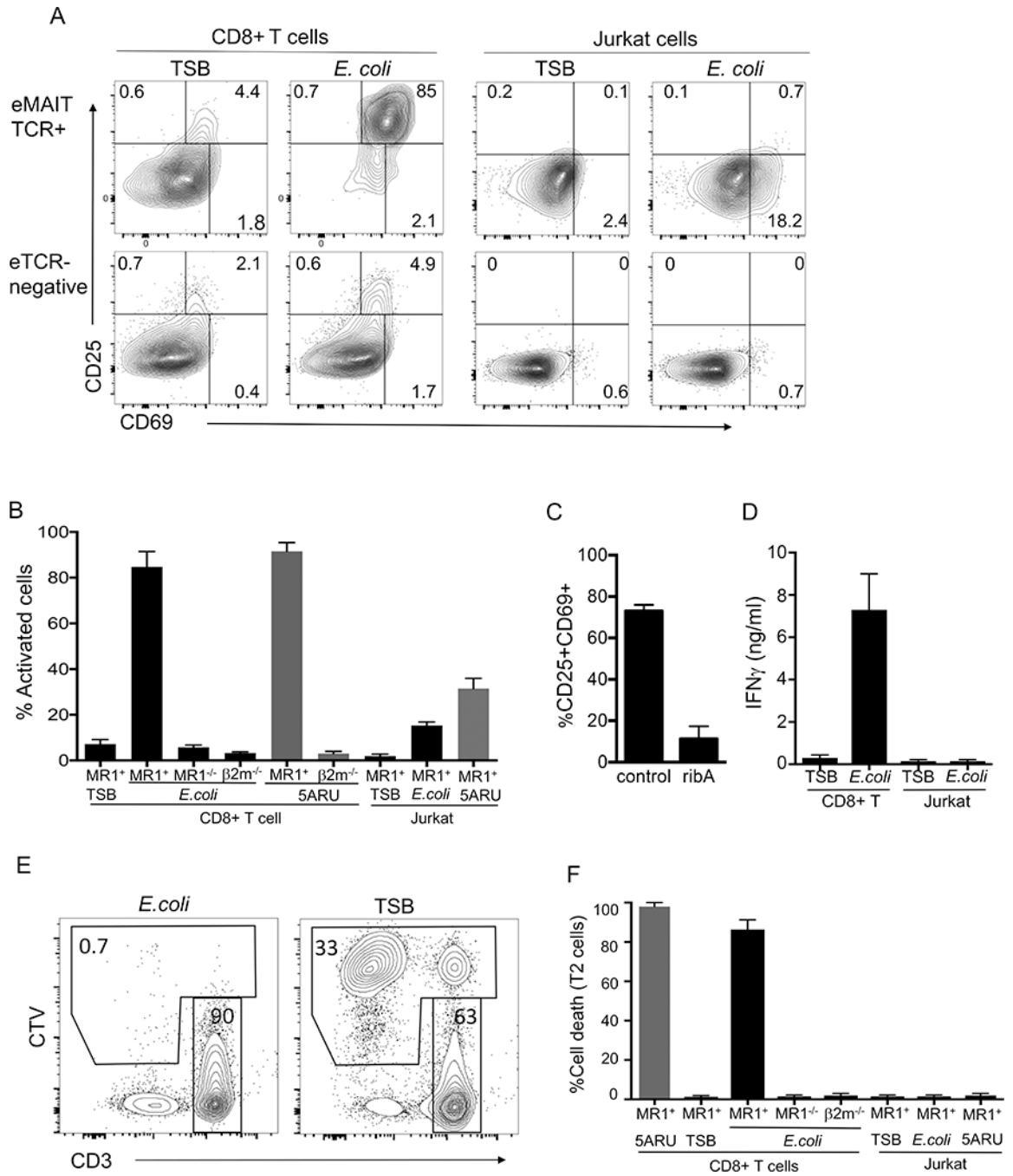
Figure 3. Effector functions of MR1-restricted eMAIT-TCR+ T cell activation.
(A) CD25 and CD69 upregulation of stimulated eMAIT-TCR-Vβ2+ CD8+ T or Jurkat cells upon culturing with T2-MR1hi cells and *E. coli* supernatant compared to eMAIT-TCR negative cells in the same culture or eMAIT-TCR+ cells in TSB control condition. (B) Quantification of the stimulated eMAIT-TCR-Vβ2+ CD8+ T cells (%CD69+ CD25+) or Jurkat cells (%CD69+) that were cultured with the T2 cells (MR1hi, MR1$^{-/-}$ or β2m$^{-/-}$) and *E. coli* supernatant, or 5-ARU compound or TSB. (C) Stimulation of eMAIT-TCR+ T cells cultured with T2-MR1hi cells and supernatants from *E. coli* clones that were transformed

with either ribA-targeting CRISPR or control non-targeting CRISPR plasmid. (D) Assessment of IFNγ secretion upon stimulation of eMAIT-TCR+ T cells using cytokine bead array (CBA). (E) FACS plots of effector CD3+ eMAIT-TCR expressing T cells and T2 cells were labeled with Cell Trace violet (CTV) fluorescent molecule (F) Quantification of the viable portion of the T2 cells (MR1^{hi}, MR1$^{-/-}$ or β2m$^{-/-}$) after culturing with eMAIT-TCR-Vβ2+ CD8+ T or Jurkat cells in the presence of *E. coli* supernatant, or 5-ARU compound or TSB. Means and standard error range of at least three independent experiments are shown.
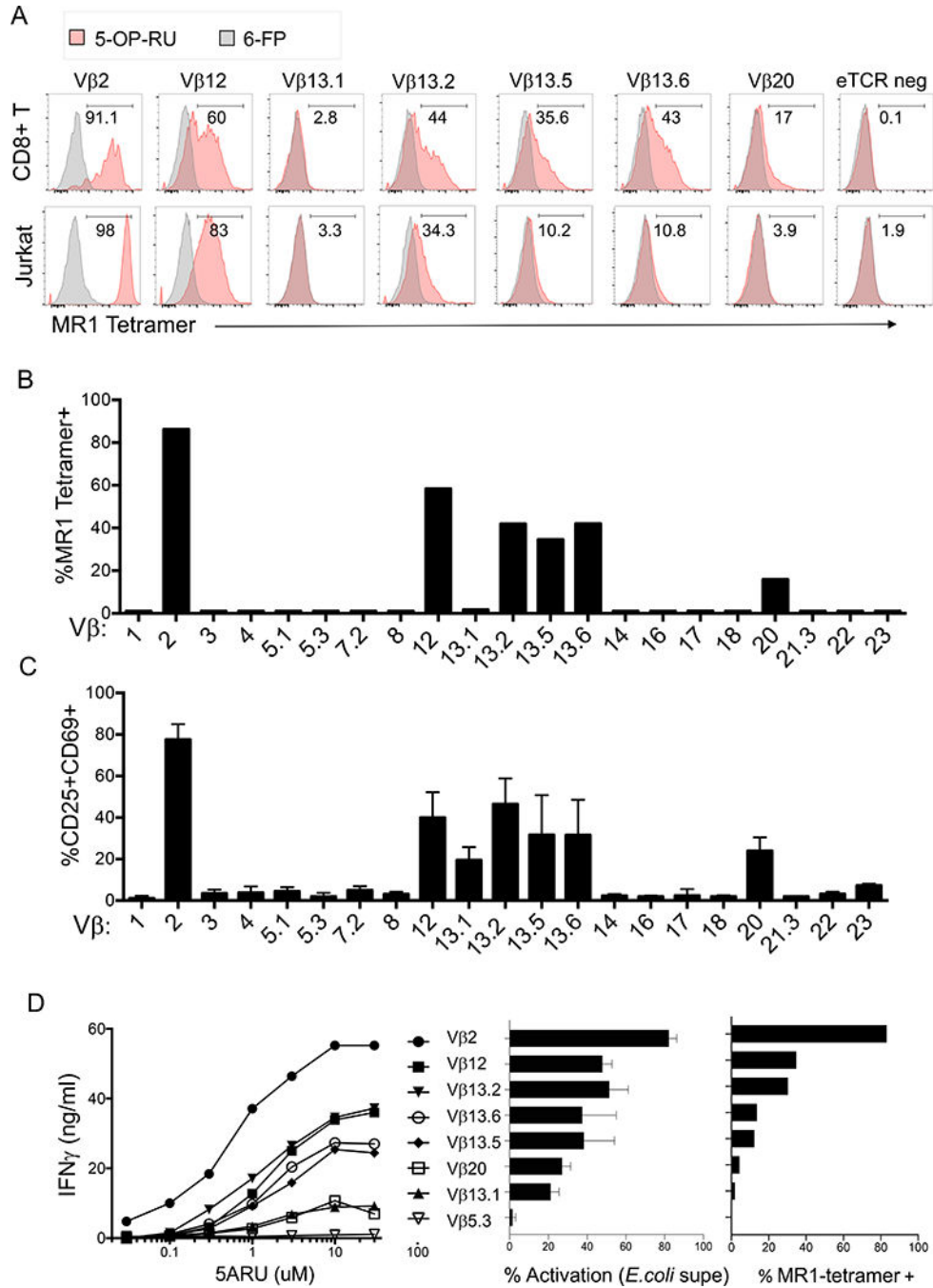
Figure 4. MRl-restricted expression and stimulation of eMAIT-TCRs.
(A) 5-OP-RU or 6-FP (negative control) pre-loaded MR1-tetramer staining of CD8+ T and Jurkat cells that express eTCRs with diverse Vβ domains after gating on GFP+ mTCRβ+ subset. (B) Quantified tetramer binding of CD8+ T cells expressing eTCRs with 21 different Vβ segments after subtracting the basal level of binding detected with MR1–6-FP tetramer staining. (C) Activation of eTCR-Vβ expressing T cells with T2-MR1^{hi} and *E. coli* supernatant, as determined by staining for CD25 and CD69 expression on T cells. (D) Activation of functional eMAIT-TCR expressing T cells with 5-ARU with T2 cells,

determined by IFNγ secretion in supernatants after 2 days of stimulation. Activation levels of each eMAIT-TCR with *E. coli* supernatant from C and quantified tetramer binding capacities of each eMAIT-TCR from B is shown on the right side of the figure corresponding to each Vβ family eMAIT-TCR for comparison. Means and standard deviation of at least three independent experiments are shown.
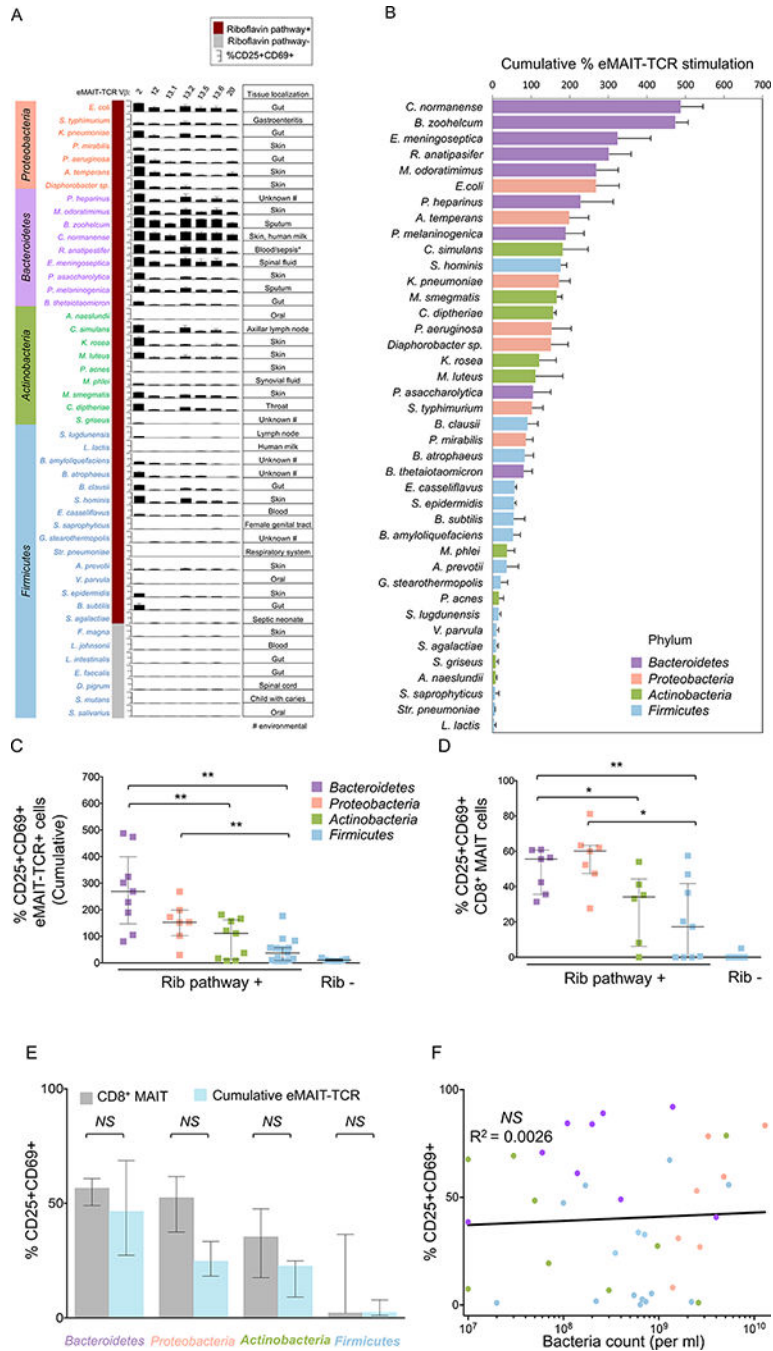
Figure 5. Screening diverse bacteria strains for their eMAIT-TCR stimulation capacity.
(A) Bacterial species clustered and color-coded based on phylum-level classification (red strip, riboflavin pathway positive strains; gray strip, riboflavin pathway negative strains). The chart plot shows CD25+CD69+ T cell percent, after each bacterial species in stimulating eMAIT- TCRs (νβ2, 12, 13.1, 13.2, 13.5, 13.6, 20) tested. Basal level of CD25+CD69+ cells was subtracted from each stimulation condition. 'Tissue localization' column indicates the places of species detected in human or found in environment (#). Means and standard error range of at least three independent experiments are shown. (B)

Cumulative eMAIT-TCR stimulation index was calculated by adding total percent stimulation of eMAIT-TCRs with 7 functional Vβ domains (Vβ2, 12, 13.1, 13.2, 13.5, 13.6, 20) from figure 5A (added to 700%) for each bacterial species possessing riboflavin pathway. The species were color-coded based on phylum. Comparison of the clustered bacterial species from different phyla by stimulation capacities of either (C) cumulative eMAIT-TCR+ T cells *(Bacteroidetes* n=9, *Proteobacteria* n=7, *Actinobacteria* n=9, *Firmicutes* n=15 and *Firmicutes* that lacks riboflavin pathway or Rib$^{-/-}$ n=7) or (D) CD8+ MAIT cells activation in PBMCs by bacteria supernatants *(Bacteroidetes* n=7, *Proteobacteria* n=7, *Actinobacteria* n=6, *Firmicutes* n=9 and *Firmicutes* that lacks Riboflavin pathway, Rib$^{-/-}$ n=5). (E) Comparison between stimulation levels of primary CD8+ MAIT cells (empty bar) and cumulative eMAIT-TCR repertoire+ T cells (cumulative activation normalized to 100% scale, blue filled) tested with same representative species from each phylum. Center line denotes sample median with interquartile ranges (*, P< 0.05; **, P< 0.01; *NS,* not significant using two-tailed unpaired Mann-Whitney rank sum U test). (F) Correlation between activation of eMAIT-TCR-Vβ2+ T cells and the bacterial numbers of the tested species having the riboflavin pathway (NS, not significant, R^2=0.0026, Spearman's rank test). Same color pallet representing different phyla was used in each of the above figures as shown in B or C.
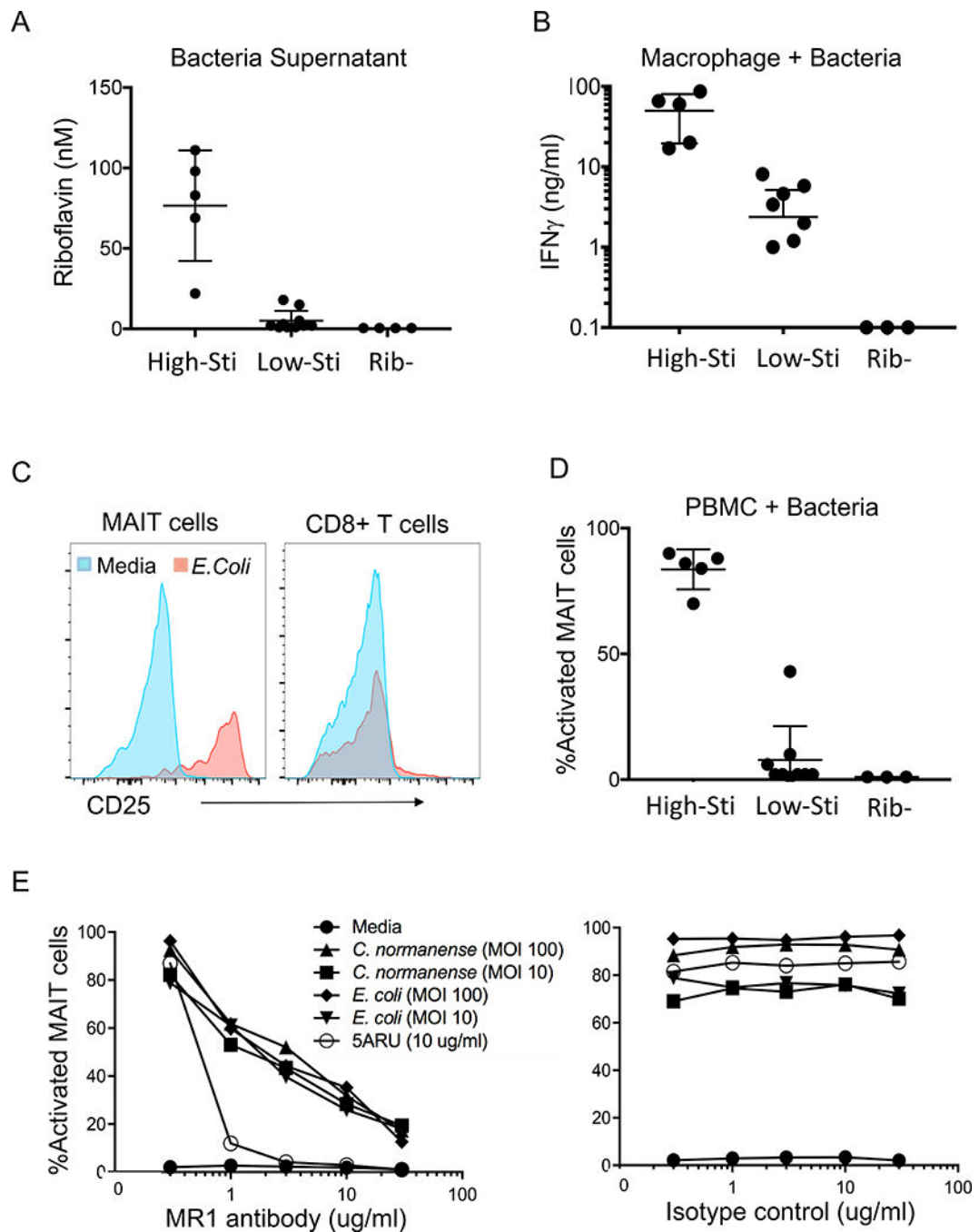
Figure 6. Stimulation of MAIT cells through antigen-presenting cells co-cultured with bacteria.
(A) Riboflavin levels in bacteria supernatants, grouped as high (n=5) or low-(n=10) stimulators (cumulative activation >200 based or <100 respectively, based on Fig. 5B) that contain Riboflavin pathway (Rib+), or those without (Rib-, n=4). (B) IFNγ secretion from eMAIT cells after 2-day stimulation with macrophages cultured in high (n=5) or low-(n=7)-stimulator or those without Rib- (n=3) bacteria (at 1:100 macrophage to bacteria ratio). (C) Activation of primary MAIT cells (gated as CD3+CD8+CD161+Va7.2+) or non-MAIT T cells (CD3+CD8+CD161-Va7.2-) after culture of PBMC with *E. coli* and (D) selected high

(n=5)- or low (n=9)-stimulator or those without Rib- (n=3) bacteria species from figure 5. (E) Blocking of MAIT cell activation by an MR1 antibody. Two high stimulatory bacteria *(E. coli and C. normanense* at MOI: 100 or 10 or 5-ARU (10 μM) were added to PBMC pre-incubated with the MR1 antibody or isotype control and activation was determined by total CD25+ CD69+ expression. Data is representative of three independent experiments with different PBMCs from healthy individuals.
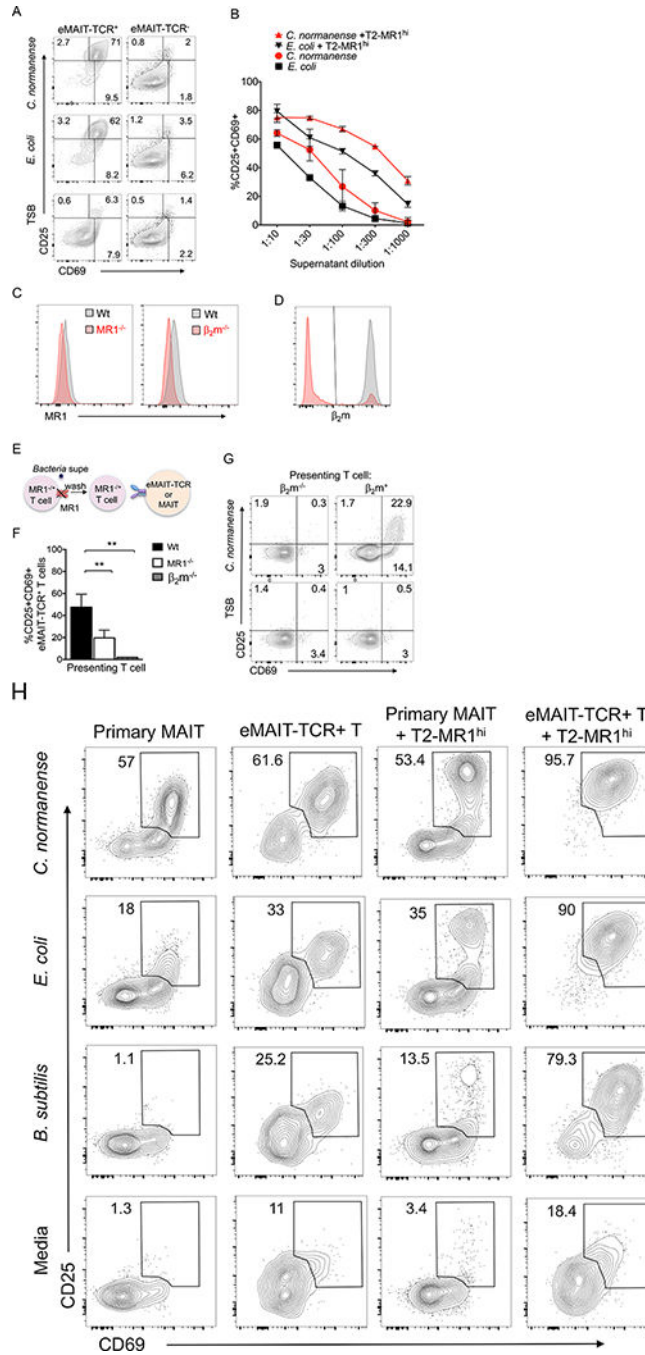
Figure 7. Stimulation of MAIT-TCR+ cells through T cell presentation of bacteria supernatants. (T2).

(A) FACS plots of CD25 and CD69 expression in eMAIT-TCR-Vβ2+ CD8+ T cells incubated with either *E. coli* or *C. normanense* supernatants and TSB control in the absence of T2 cells. (B) Quantitative stimulation of eMAIT-TCR+ T cells in the presence or the absence of T2-MR1hi cells with dose-dependence of *C. normanense* (red lines) or *E. coli* (black lines) supernatants after subtracting basal level of CD25+CD69+ of eMAIT-TCR+ T cells incubated with TSB. (C) Expression of MR1 on T cells that were either wild type (Wt, gray), MR1-deleted (MR1−/−, red) or β2m-deleted(β2m−/−, red) T cells. (D) β2m expression

in Wt or β2m$^{-/-}$ T cells. The β2m-negative (deleted) T cell subsets were sorted as shown (red portion). (E) Experimental setup to assess stimulation of either eMAIT-TCR+ T cells or MAIT cells in the purified CD8+ T cells that were cultured with CD4+ or CD8+ T cells (wt, MR1$^{-/-}$ or β2m$^{-/-}$) preincubated with *C. normanense* supernatant. (F) Quantification of the activation level of eMAIT- TCR$^+$ T cells via the T-MAIT cell stimulation after subtracting basal level of CD25+CD69+ in TSB (*, P< 0.05; **, P< 0.01 using two-tailed unpaired Mann-Whitney rank sum U test). (G) CD25 and CD69 expression in the primary MAIT cells within purified CD8+ T cells cultured with sorted β2m$^{-/-}$ or β2m$^+$ CD4+ T cells. (H) CD25 and CD69 expression in primary MAIT cells in purified CD8+ T cells and eMAIT-TCR-Vβ2+ T cells in presence or absence of T2-MR1^{hi} cells pre-incubated with *C. normanense, E. coli, B. subtilis* supernatants or control growth media (TSB or nutrient broth). Percent of activated T cells (CD25+CD69+) are shown in each plot.
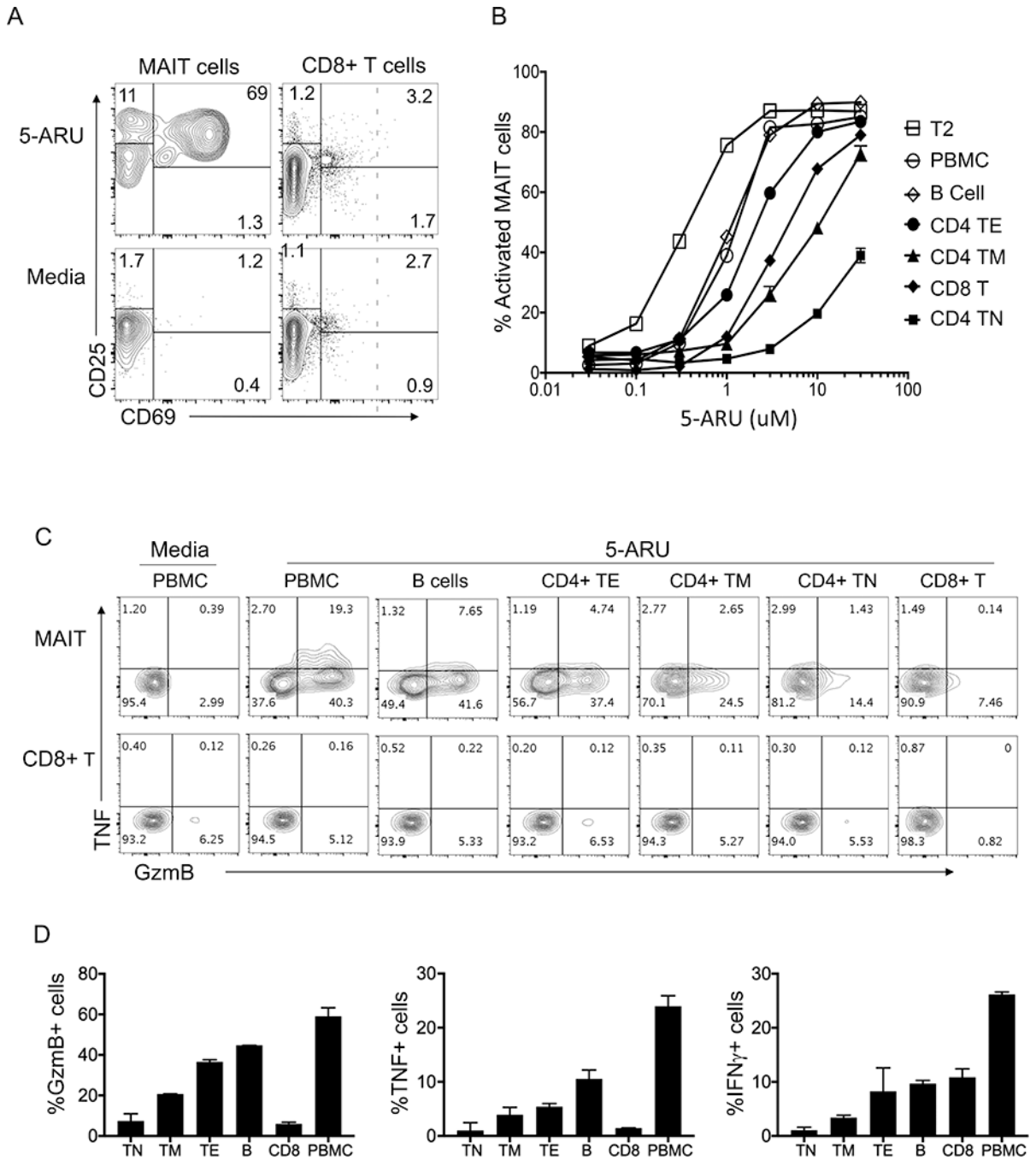
Figure 8. Activation thresholds of MAIT cells through MRI-restricted 5-ARU compound presented by T cell subsets.

(A) Activation of MAIT cells in PBMC (gated as CD3+CD8+CD161+Va7.2+) or non-MAIT cells (gated as CD3+CD8+CD161-Va7.2-), assessed by CD25 or CD69 expression after 2-day incubation with 10 μM 5-ARU. (B) Activation of MAIT cells (CD25+ CD69+ cells) after stimulation with CD4+ T cell subsets, naïve (TN), memory (TM), effector/activated (TE) and B cells pre-incubated with different concentrations of 5-ARU, washed and added to PBMC that contained MAIT cells (~2%). The compound was also added directly to PBMC (shown as PBMC) or purified CD8+ T cells that contain most MAIT cells. (C) PBMCs

activated as in B, were stained intracellularly for Granzyme B (GzmB), IFNγ and TNF along with cell surface markers to define MAIT cells, data shown are cells gated on MAIT cells (CD3+CD8+CD161+Va7.2+) or non-MAIT cells gated as (CD3+CD8+CD161-Va7.2-). (D) Analysis of data from 8C, as proportion of MAIT cells that express GzmB, TNF or IFNγ (after subtracting background of non-stimulated cells) upon stimulation different cell types. There was no difference between the background and after stimulation in non-MAIT T cell subsets in the same PBMC (data not shown). Data is representative of three independent experiments with different PBMCs from healthy adult donors.